FINAL REPORT
TACSEA CLUTTER MEASUREMENT VERIFICATION

29 October 1976

N00017-72-C-4401

Technology Service Corporation

DISCLAIMER NOTICE

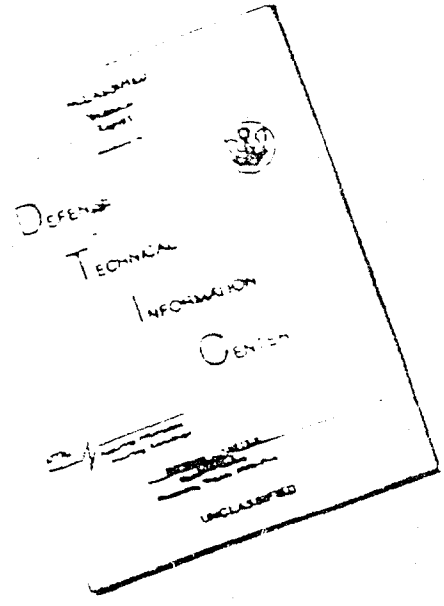

THIS DOCUMENT IS BEST QUALITY AVAILABLE. THE COPY FURNISHED TO DTIC CONTAINED A SIGNIFICANT NUMBER OF PAGES WHICH DO NOT REPRODUCE LEGIBLY.

Technology Service Corporation

Washington Operations: 8555 Sixteenth Street, Silver Spring, Maryland 20910 Phone: [301] 565-2970

TSC-WO-284R
B50711

FINAL REPORT
TAGSEA CLUTTER MEASUREMENT VERIFICATION

29 October 1976

APL Contract 600486

L. W. Brooks
F. E. Nathanson
P. R. Brooks

Submitted to:

Applied Physics Laboratory
Johns Hopkins University
Laurel, Maryland
Attn: John Cullens/David Belt

CONTENTS

Letter on file

A

1.0 SUMMARY AND CONCLUSIONS

This is the final TSC report on our overview of the TAGSEA sea clutter measurement program. It includes some general comments on the techniques used by Raytheon and General Dynamics in obtaining the data, the data reduction, and test results. Since the early discussions on procedures and tests were covered in monthly meetings and reported earlier, this report emphasizes the validity of the results and their use in relating sea clutter model for Navy use.

TSC has no reason to question the validity of the data itself. While the system was not designed for quantitative measurement of σ_o, the results should be accurate to within a few decibels [± 3 dB(2σ)]. Both Raytheon and General Dynamics appear to have performed good tests in the time allotted. Two areas deserve special attention.

1.1 Conclusions on Reflectivity

While the measurement of sea reflectivity, σ_o, was not a primary function of the tests, the results showed the greatest deviation from earlier models. For grazing angles of $10° < \psi < 45°$, the TAGSEA mean values of σ_o were 6-9 dB higher than earlier models, especially those of NRL for the higher sea states (SS>4). It is proposed in Section 3 that TSC believes that the TAGSEA results are probably more representative of high sea state reflectivity than the earlier models and that some values in new "models" should be raised by 4-6 dB. This conclusion is not solely based on TAGSEA results, but also on other recent experiments by several capable experimenters.

As expected, the reflectivity was higher on vertical than horizontal polarization. Reflectivity was higher in the upwind direction than in the cross-wind direction as in earlier tests. However, the downwind reflectivity data was about equal to the upwind TAGSEA data. Some earlier data indicate larger upwind/downwind ratios for horizontal polarization.

1.2 Conclusions on Statistics

The TAGSEA statistical fluctuation model appears to be a good engineering design model. There, the total fluctuation is given as the product of three processes:

$$\sigma_o = \bar{\sigma}_o \cdot F \cdot S$$

where $\bar{\sigma}_o$ is the average cross-section

S is a slowly fluctuating process representing long-term, large-spatial fluctuations in the cross-section

and F is a fast fluctuation process which has a non-Rayleigh distribution.

The above model is consistent with a time-varying Rayleigh (TVR) fluctuation model which has been proposed by several authors and developed in some detail by Sodergren [8] and Trunk [22]. In the TVR model, the primary scattering mechanism is Bragg scattering from (small scale) capillary waves. The variable nature of the slow fluctuations arises from local tilt produced by the (large scale) gravity waves and by variations in the local wind field. A usual application of the TVR distribution models the fast fluctuation as a Rayleigh process. Such application, however, ignores the difficulty in obtaining independent samples from the same range cell under "frozen" conditions. That is, under conditions such that the local tilt or wind field does not change during the sampling interval. The TAGSEA model provides a hedge against this mistake by lumping some of the non-Rayleigh characteristics into the fast fluctuations.

As noted in [1], the model is limited to a fairly specific set of conditions -- high-resolution radar, high sea state, and moderate grazing angle. Comparison with other data indicates that at low grazing angle the σ_o fluctuations have much higher tails (2-8 dB at 10^{-5} probability of a threshold crossing) and show fairly strong dependence on sea state. The TAGSEA model should only be applied to conditions similar to the data set from which it was derived. Comparison with the NRL 20 nsec radar indicate that a higher resolution radar may produce higher tails than the TAGSEA model. Thus, a conservative design practice would be to design to a somewhat more severe model (e.g., 1-2 dB higher tails at 10^{-4}).

Theoretical calculations, Sodergren's model, and the TAGSEA model differ on the rate of rapid fluctuations. For coherent frame rates that are of the same order as the fast decorrelation time, both the amplitude distribution of clutter signals (which affect detection thresholds) and second order statistics (which affect MTI/Doppler processing) would depend on the integration and decorrelation processes.

2.0 TECHNOLOGY SERVICE CORPORATION TASKS

TSC's role in the TAGSEA program was divided into two areas. The first role occurred during the measurement and algorithm development phases. It consisted of reviewing the objectives and plans in both of these areas. The mode of operation was primarily by direct technical discussions on a monthly basis. These are summarized in minutes of those meetings.

The second role occurred both during and after the measurements and consisted of reviewing the data as available from Raytheon and supplying them with existing models for them to check their initial results. The review of the Raytheon final report is given in Section 3.0 of this report.

The TSC tasks are shown below:

A. "TSC will review the Raytheon Test Objectives and Test Plan to insure that the data obtained will contain adequate information to determine the desired sea clutter statistics. This will include TSC evaluations of the PRF and the number of independent samples, dynamic range optimization, allowance for aircraft motion, polarization properties, sufficiency of the number of samples and sea conditions within the constraints of the overall program.

"TSC will review the instrumentation and especially the calibration techniques. TSC will help insure that the critical problem of obtaining sufficient sea state descriptors are in the planning at the time of the tests.

"TSC will review the data reduction techniques in the critical areas of obtaining distribution functions for both small areas resulting from beam sharpening in azimuth, and the larger regions defined by the azimuth beamwidth.

B. "TSC will interpret the results in the light of Navy requirements. Verification of the results will be performed both by reviewing the procedures, data reduction and analysis described in Tasks 1 and 2 and by comparing certain results with earlier reflectivity models developed by NRL, TSC, APL and others. In addition, the measured distributions will be checked against models developed by NRL (Trunk), APL (Sodergren) and in unpublished TSC reports."

A Final Report will be issued that includes verification of the Raytheon results and comparison with other models.

- - - - - - - - - - - -

TSC personnel attended meetings at Raytheon on

12 January 1976
25 February 1976
12 April 1976
11 May 1976
22 June 1976
30 July 1976

plus several meetings at APL/JHU. TSC memos related to these meetings are available [25, 29, 30, 31, 32, 33].

2.1 Validation of Test and Data Reduction Procedures

In general, the constant interaction between APL/JHU, General Dynamics, TSC and Raytheon, Bedford achieved a set of test procedures and data reduction techniques that were acceptable to all parties. It must be pointed out that the distributions presented are describing a non-stationary process, and there is no established "right" or "wrong" in the selection of observation times, number of samples, and spatial averaging.

TSC would have preferred slightly more emphases on distributions of a single spatial cell, but this does not seem to have affected the conclusions.

TSC would like to have obtained more data on horizontal polarization and at lower grazing angles, but the short time scale and equipment limitations did not permit this.

3.0 VALIDATION AND INTERPRETATION OF RESULTS

This section relates the reported Raytheon data to both prior experiments and theory. This section is split arbitrarily between mean reflectivity, σ_o (or σ^o), and sea clutter statistics. However, a revised theoretical model for reflectivity is included in the statistics section.

3.1 Reflectivity of Sea Clutter

While sea clutter reflectivity measurements have been performed for over 30 years, controversy remains in both the reflectivity and statistical models in some specific areas. The general rules and their limitations for grazing angles of 1°-40° can be summarized as follows for a fully developed sea:

a. The monostatic backscatter coefficient, σ_o, monotonically increases with grazing angle, ψ, from below 1° to above 40° for all sea states, with a higher slope from 1°-10° and a lesser slope from 10°-40° (depending on frequency and sea state).

b. The backscatter coefficient monotonically increases with sea state with a higher slope at lower grazing angles, lower carrier frequencies, and lower sea states. The rate of change of σ_o decreases at the higher sea states. There have been claims that at the higher frequencies (f_o>5GHz) there is a "saturation" at about Sea State 4. This is the subject of active controversy between NRL [26, 34] which believes in saturation and NASA related experimentors and theoreticians [5, 12] who are estimating wind speed (and sea state) from reflectivity for satellite radar programs. The NASA experiments and related theory by Pierson show no saturation up to about Sea State 7.

c. The reflectivity increases monotonically with carrier frequency, f_o, from 0.5 GHz to at least 5.0 GHz. It also appears that σ_o decreases with frequency from f_o<35 GHz to over f_o=100 GHz. At this point there is again controversy with NRL measurements at high sea states tending to decrease

at 10 GHz from measurements at 5GHz while other experiments show σ_c increasing with frequency to above 10 GHz and perhaps to 15-18 GHz or even 35 GHz.

d. The mean reflectivity on vertical polarization exceeds that of horizontal polarization for $1° < \psi < 40°$, and virtually all sea states for carrier frequencies of 0.5 to about 15 MHz. The amplitude distribution is also closer to a Rayleigh distribution for vertical polarization than is the more "spiky" horizontal polarization. Thus, a caution must be attached to using the lower values of σ_o on horizontal polarization (σ°_{HH}) when automatic detection circuitry is contemplated. False alarm problems may develop when attempting to detect small aircraft or ships in a spiky sea clutter background. Fig. 3.1 illustrates the effect using the Raytheon "TAGSEA Extreme Model". The ordinate is the probability that σ_o exceeds the values on the abscissa. The important point is that while in this example, the median value of σ_o is 6 dB lower for σ°_{HH} than for σ°_{VV}, the receiver threshold level required to limit the clutter false alarm probability to 10^{-5} differs by only 2 dB. Further information on these statistics is given in Section 3.2.

e. The reflectivity is higher when looking upwind rather than crosswind. These values are typically 2-6 dB. Downwind values are generally between the two, but closer to the upwind value. NASA and NRL reports have considerable measured data with some in a recent Boeing Report [9].

Note that all of the above refer to the grazing angle of the EM radiation and not the depression angle of the radar aperture. Note also that the data is primarily for pulse durations, τ, greater than 0.25 microsecond or 125 ft in radial extent. Effects of beamwidth or azimuthal extent are suspected but not found to date.

Without TAGSEA data, there was controversy about the mean values and the statistics in certain situations. The TAGSEA experiments provided additional data. These are presented in the next section.

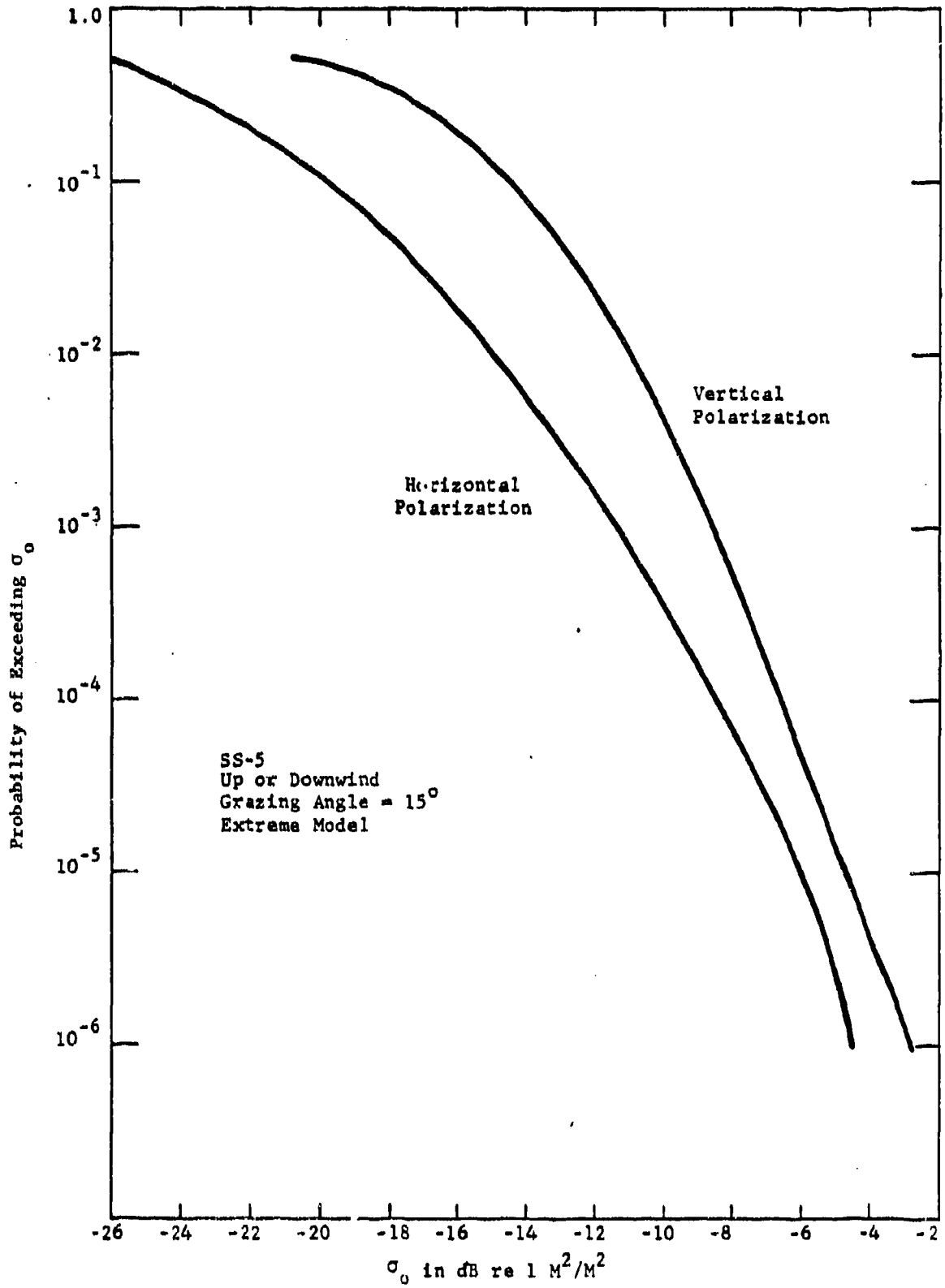

Figure 3.1. Sea Clutter Amplitude Distributions-TACSEA Model.

3.1.1 TAGSEA Results and Data Comparison

The TAGSEA data on reflectivity can be summarized quite easily:

frequency	=	X-Band
grazing angles		$4.7° < \psi < 52.8°$
polarization	=	both linear polarizations (more vertical data than horizontal)
resolution	=	118 ft effective in range and varying in cross range, but typically 100'
sea state	=	1 to 5 + with reasonable receiver signal-to-noise ratios at the higher sea states

The results for σ_o were self consistent from run to run, and for measurements in the Atlantic and Pacific Oceans. The values of σ_o were consistently 6-10 dB higher than the NRL 1965-1969 data which forms most of earlier data base.

The summarized Raytheon TAGSEA results from Fig. 4-8 of BR-9254-1 Volume I [1] are shown on Fig. 3.1-1 along with the earlier TSC projections for the same conditions. Note the consistently higher reflectivity values from the TAGSEA tests.

It must be pointed out that the earlier TSC models are to a great extent the NRL data taken from the 4FR aircraft in the 1960's. The number of data points from this aircraft was so great that it far outweighs other data points at X-Band carrier frequencies.

Some of the NRL data points for ψ=10° ψ=30° are illustrated on Figures 3.1-2 and 3.1-3. While the concept of a "saturation" in σ_o as sea state increased to about SS4, bothered a lot of theoreticians, the reliability of the equipment and general care in calibration led people to choose the experimentally derived models.

However, in the early 1970's, NASA was engaged in a program to measure wind speed by sea reflectivity measurements using a "scatterometer", a radar technique to estimate σ_o. These were part of the SKYLAB and SEASAT programs. If the saturation theory was correct, their device could not predict high winds

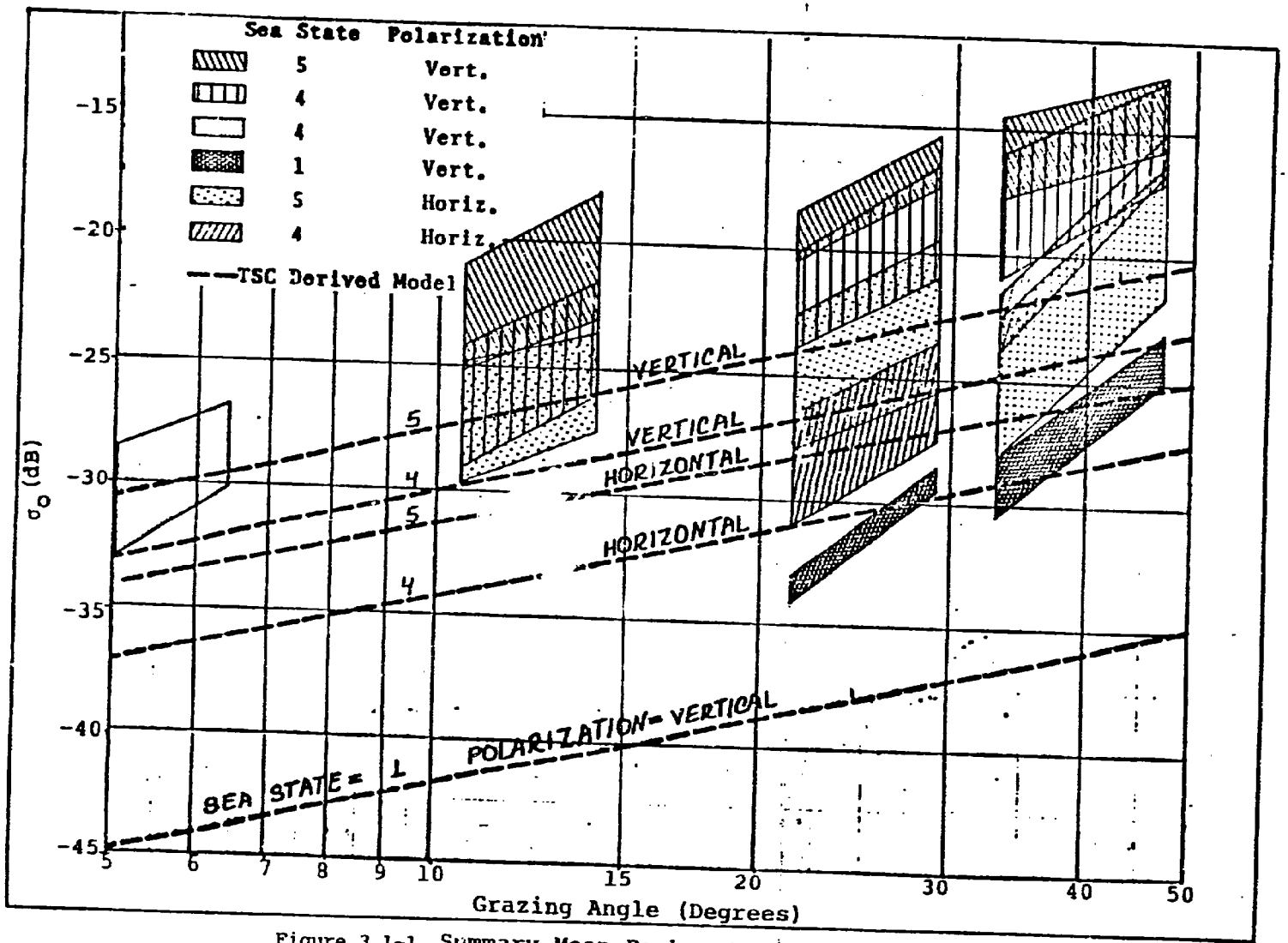

Figure 3.1-1. Summary Mean Backscatter Coefficient

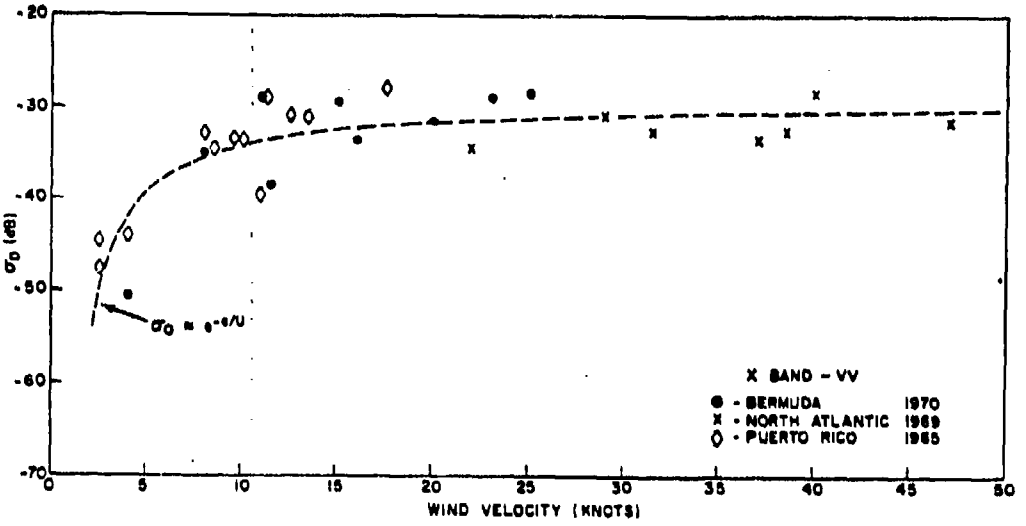

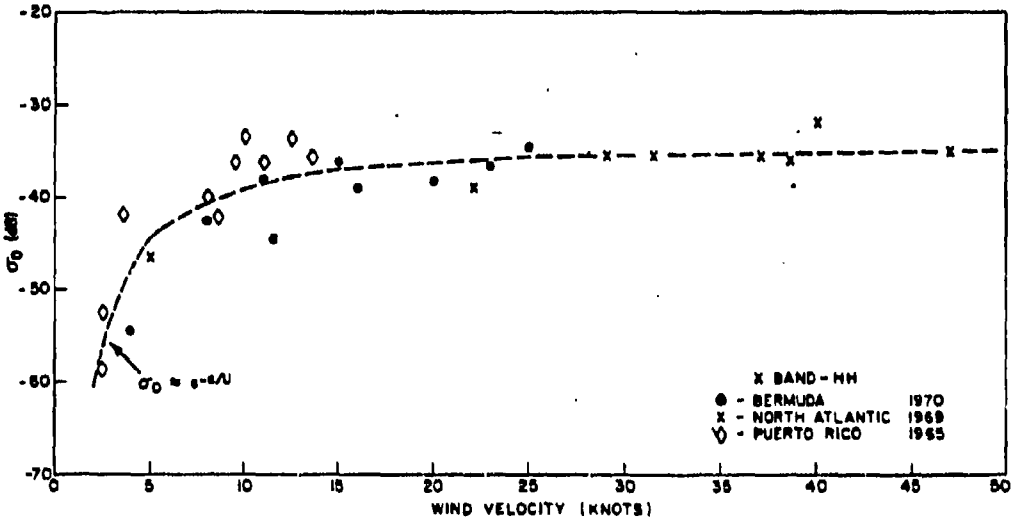

Fig. 3.1-2- Median NRCS of the sea vs wind velocity; X and ● bands upwind, 10° depression angle

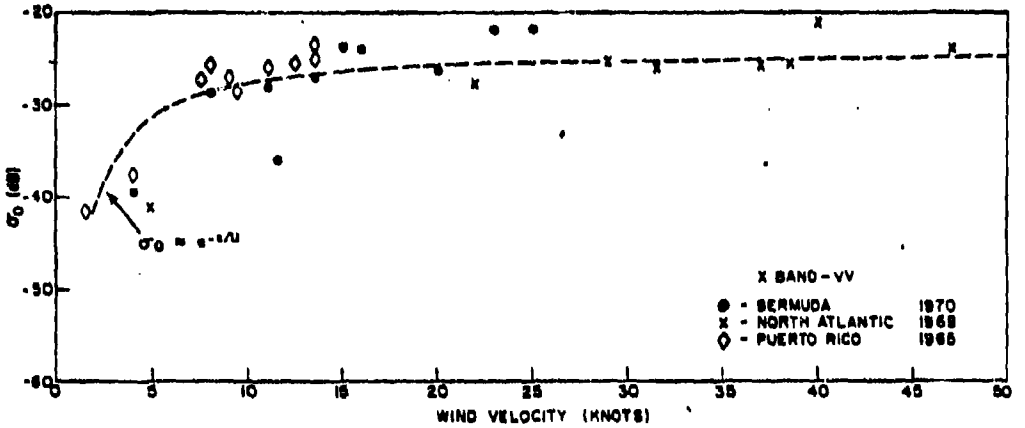

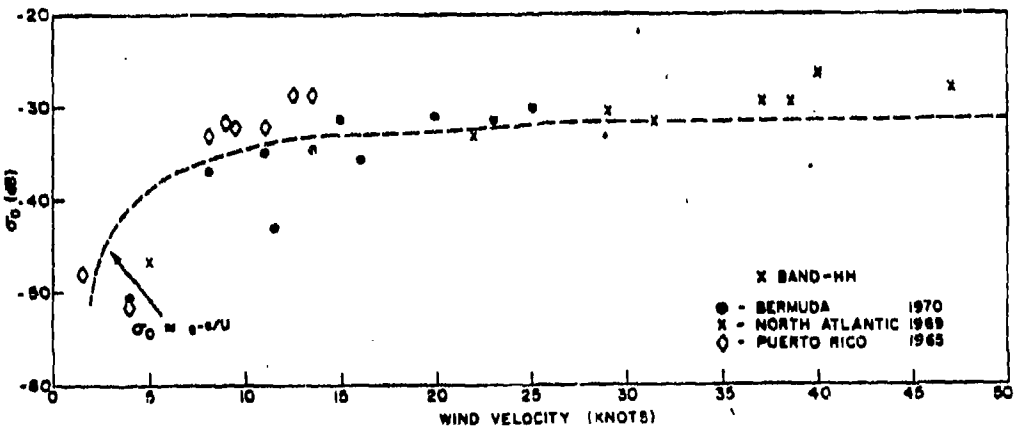

Fig. 3.1-3 - Median NRCS of the sea vs wind velocity; X and ● bands upwind, 30° depression angle

(or high sea states). NASA, with the University of Kansas, flew many flights of a K_u-Band radar (13.9 GHz) to measure σ_o vs wave height and wind speed. They also engaged Dr. Willard Pierson of NYU to relate radar echoes to oceanographic parameters. The NASA data and related theories did not exhibit the saturation. Thus, two extensive sets of data existed with the only difference being the carrier frequency difference between 9.5 and 14 GHz.

In order to validate the TAGSEA results, the NASA data, along with the NRL and TAGSEA results and other recent measurements, are graphed on Figures 3.1-4 and 3.1-5 for Horizontal and Vertical polarization. The primary difference with other earlier graphs is that high sea state data points at several carrier frequencies are shown on the same graph.* Also included are APL data points [8, 35] that had not heretofore been available to TSC, and recent S-Band measurements by Boeing Aircraft Corporation [9]. Note that the X- and K_u-Band data show little difference except that now the NRL σ_o data seems low. The 10 dB lower values for the Boeing S-Band data can probably be explained by the factor of 3 difference in carrier frequency.

Thus, the saturation effect of the NRL data appears to be violated by several experiments including TAGSEA. Since the NASA data set, which is the second most extensive, was acquired at a somewhat higher carrier frequency and only overlaps the NRL data at the higher grazing angles, it alone would not be sufficient to alter the models. However, the additional APL data at both X- and K_u-Bands and the Sittrop data [28] seem to confirm the higher values for σ_o at high sea states and that there is little difference in σ_o between X- and K_u-Band. APL 72 refers to references [23] and [35].

Some care must be used in interpretation since σ_o is generally given as a mean value while NRL generally publishes a median value. The Boeing data is also a median value. The mean-to-median ratio is typically +1.6 to 2.0 dB, for the angles of interest, and perhaps higher at the lower grazing angles. This has the effect of raising the NRL and Boeing data and closing the gap. A model is discussed in the next sections.

---

*The winds were all in excess of 22 knots with the exception of the APL Tests.

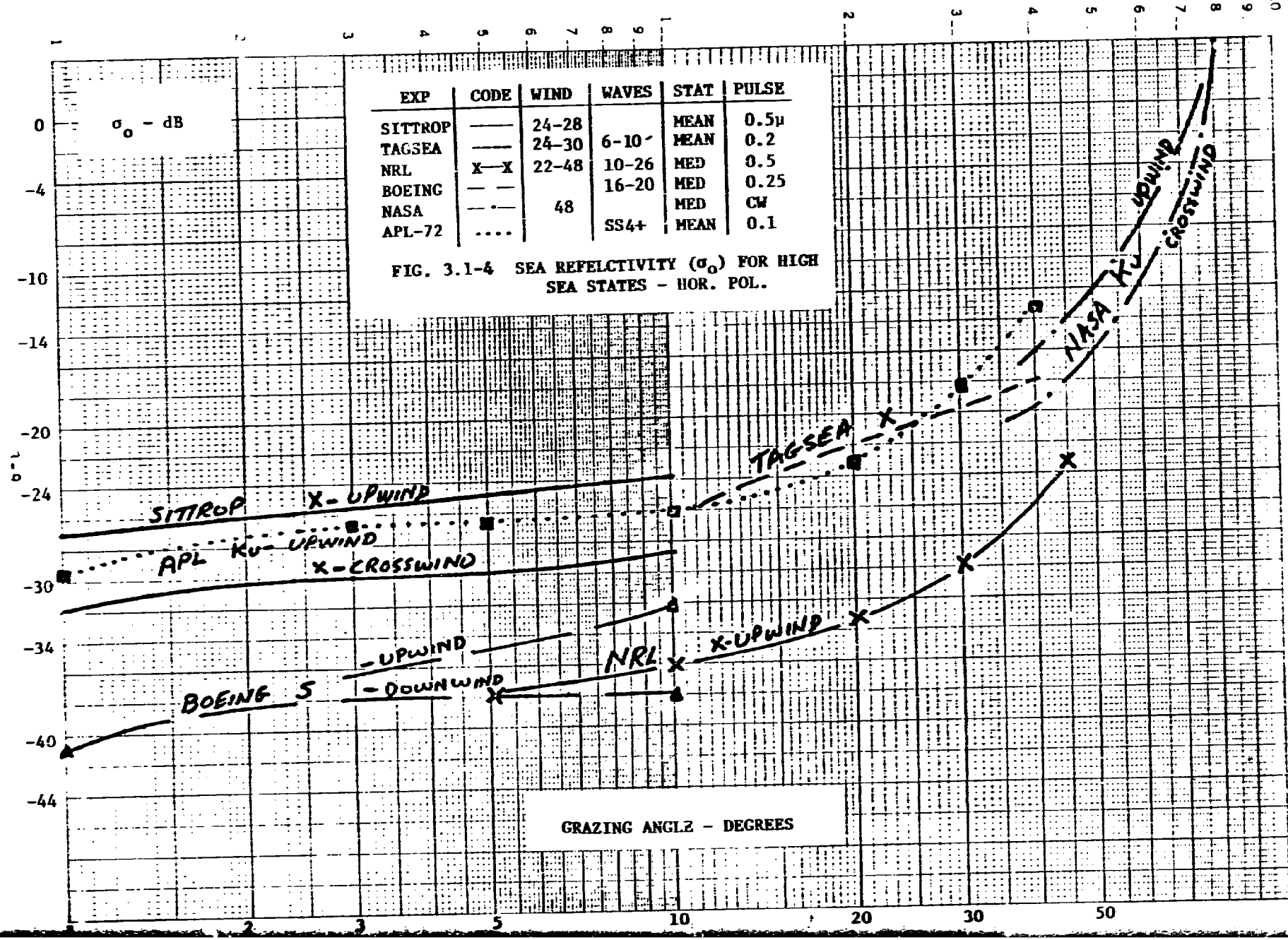

EXP	CODE	WIND	WAVES	STAT	PULSE
SITTROP	——	24-28		MEAN	0.5μ
TAGSEA	——	24-30	6-10′	MEAN	0.2
NRL	X—X	22-48	10-26	MED	0.5
BOEING	— —		16-20	MED	0.25
NASA	— ·—	48		MED	CW
APL-72	....		SS4+	MEAN	0.1

FIG. 3.1-4 SEA REFELCTIVITY (σ_o) FOR HIGH SEA STATES - HOR. POL.

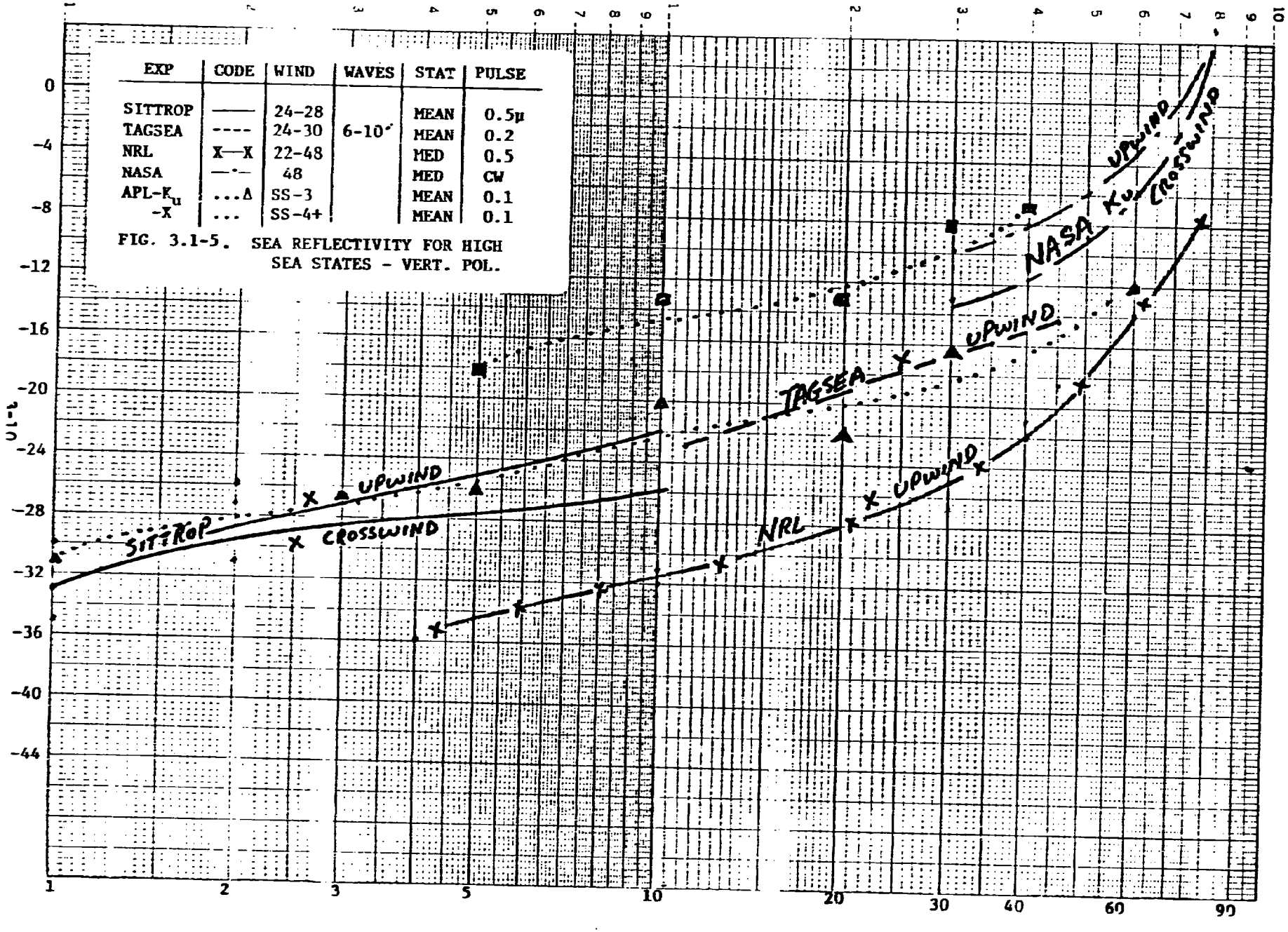

FIG. 3.1-5. SEA REFLECTIVITY FOR HIGH SEA STATES - VERT. POL.

3.2 Evaluation of the TAGSEA Model of Sea Clutter Statistics

In this section, the validity of the statistical fluctuation model proposed in reference [1] is examined. Although absolute validity is extremely difficult to establish, it is possible to examine the correspondence between the model and existing information about the reflectivity of the sea surface. Generally, a model should be consistent with accepted theory of backscatter from a rough surface, and should agree with experimental measurements. If the model satisfies these criteria, then until an improved theory is developed, or new experimental observations are made, it is usually accepted as a valid characterization. In the following sections, these aspects of the TAGSEA fluctuation model are examined.

Generally it is found that the TAGSEA model agrees well qualitatively with a time and space varying Rayleigh distribution. Such a model can be derived from a composite sea surface model for which gravity waves tilt the local surface seen by the radar and for which the primary scattering mechanism is Bragg scattering from capillary waves. In addition to qualitative agreement, significant quantitative agreement exists for vertical polarized cases when the Pierson and Stacy [5] sea surface model is used. Since that model was derived largely from direct water-wave measurements rather than radar measurements, the agreement tends to validate both models.

A comparison with experimental data indicates that most previously reported data has been taken at low grazing angles and is not appropriate for comparison with the TAGSEA model. Four references, [6]-[9] were available to provide high-resolution, moderate-grazing-angle, and high-sea-state data for comparison with the TAGSEA model. Of these data, measurements from the NRL 20 nsec radar gave distribution functions for the cross section fluctuation which had significantly higher tails than the model. The Boeing data was too preliminary for detailed comparison but appeared to give results similar to the TAGSEA model. Sodergren's results provided the closest agreement with the model.

Generally the model proposed in [1] appears to be good for engineering design and evaluation. As was noted in [1], it was derived for a specific set

of conditions — high-resolution-radar, moderate-grazing-angle, and high-sea-state. Comparison with data taken at low grazing angle [8], [10], [11] indicates that significant modification of the model is required at low grazing angle. In this case, the model for fluctuation statistics will be sea state dependent, and will generally have significantly higher tails than the TAGSEA model (e.g., as much as 2-8 dB at the 10^{-5} point, depending on sea state).

No consistency has been found for determining the rapidity of the fast fluctuations. The TAGSEA model, Sodergren's model and the theoretical discussion of Section 3.2.1 all give different relations for the bandwidth of the fast fluctuations. For low data rate systems (frame rate <100 Hz) this is not important since all the above models degenerate to independant fluctuations. For very high data rate systems, the problem will become significant and should be investigated.

3.2.1 Comparison Between the TAGSEA Model and Rough Surface Scattering Theory

Theoretical models for scattering from rough surfaces have been studied by many investigators both from the standpoint of electromagnetic scattering from above the sea surface and acoustic scattering from below. The references on the subject are extensive, and those listed [12]-[16] represent only a small sample. In the reference list, Swift and Jones [12] give a nice, simple discussion of electromagnetic scattering from the sea surface. Peake and Oliver [13], Barrick [14], or Barrick and Peake [15] have more comprehensive discussions. Horton and Muir [16] give a good summary of the theory of acoustic scattering from the sea.

The theoretical model that appears to be gaining the widest acceptance, especially in remote sensing and satellite-radar-scatterometry, is the composite surface model (see Peake and Oliver [13], pg. 74-77). In this model, the ocean surface is characterized as the sum of two independant processes - a large scale roughness, which has a small scale roughness superimposed. Wright [24] has applied this model to a series of radar measurements. For scattering at X and K_u band, the large scale roughness is approximately associated with the gravity waves and swell, while the small scale roughness is associated with the capillary waves.

Generally "large scale roughness" is defined to mean that the surface height variations are large relative to the radar wavelength. Scattering from this scale can be computed when the surface is gently undulating so that the curvature is always much greater then the radar wavelength, and the slopes of the surface are small. When these conditions hold, the scattering properties can be obtained by computing the number and curvature of the specular points as is illustrated in Fig. 3.2-1 (Peake and Oliver [13]). Barrick [14] has analyzed this case in some detail, and has derived mean cross section as well as cross section statistics.

For a rough surface, the mean cross section is given by

$$\sigma^o = \frac{|R|^2 \sec^4 \theta}{S^2} \exp\left[-((\tan \theta)/S)^2\right] \qquad (1)$$

where

θ is the angle of incidence, i.e., the angle between the look direction and the normal to the surface

$|R|^2$ is the power reflection coefficient of a plane wave normally incident on a flat dielectric surface (at X band $|R|^2$ is approximately -2.1 dB for sea water)

and

S^2 is the rms slope of the surface.

The normalized cross section versus incident angle is given in Fig. 3.2-2 for a Gaussian surface as a function of the rms slope.

For a fully developed sea surface, Swift and Jones [12] give the rms slope as a function of wind velocity in meters per second as:

$$\begin{aligned} S^2 &= (3.16 \times 10^{-3})\ V \quad \text{(up/down wind)} \\ &= .003 + .00192\ V \quad \text{(cross wind)} \end{aligned} \qquad (1a)$$

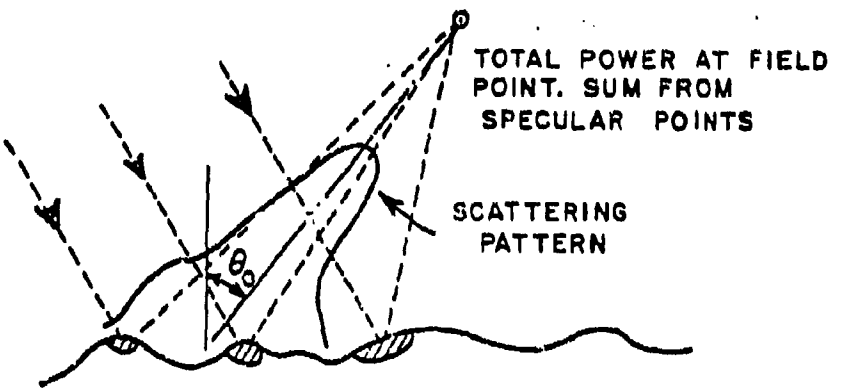

Figure 3.2-1. Scattering from an Undulating Rough Surface; $h \gg \lambda$, slopes $\ll 1$, scattered beamwidth $\approx$ rms surface slope, specular. (from [13])

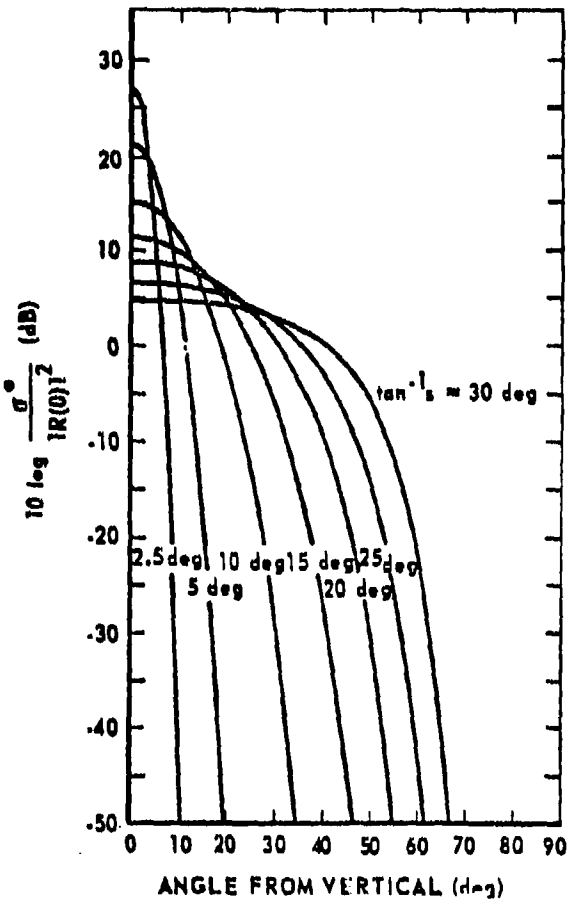

Figure 3.2-2. Average Radar Cross Section per Unit Surface Area σ^{o} for Very Rough Gaussian Surface. (from [14])

Note that for sea state 5, a typical wind velocity is about 11 m/s (22 knots); this gives an rms slope of about 10°. From Figure 3.2-2 one would expect the rough surface scattering cross section to be small at incidence angles greater than 30 degrees. All the TAGSEA results correspond to higher angles of incidence; thus the specular scattering model which applies near vertical incidence would not be expected to apply to the TAGSEA results.

The small scale roughness is defined to be those height variations which are much smaller than the rf wavelength. The scattering mechanism from this component of the surface is completely different than the rough surface scattering discussed previously. The case of a slightly rough surface, can be computed by a perturbation technique described by S.O. Rice [17], the first order coefficients have been developed in detail by Barrick [18].

In general, the total field produced by a slightly rough surface is the sum of a coherently reflected and a diffusely scattered component as sketched in Fig. 3.2-3. The coherent component is identical to the field reflected from a perfectly flat surface, but the power has been reduced by the factor $\exp(-2(kh\cos\theta_i)^2)$ where k is the rf wave number, and h is the rms surface height. The first order expression for the diffuse component can be shown to be equivalent to the Fourier transform of the surface height.

A useful concept for understanding the characteristics of the diffuse component is to consider each point on the slightly rough surface as a nearly isotropic scattering point. The field which is reradiated is proportional to the incident field, but the phase is determined by the height of the surface. Such a surface acts as a "phased array" with small random phase errors which are proportional to the height of the surface. Since the array is "fed" by the incident plane wave, it is phased so that the maximum response is in the specular direction. The diffuse component corresponds to sidelobes produced by the random phase errors. For small enough phase errors (i.e., a slightly rough surface), the sidelobe response is proportional to the Fourier transform of those errors. Note that the diffuse component is not the result of many <u>independent</u> point scatterers, since the phase and amplitude of each point on the surface is determined by the incident and look directions,

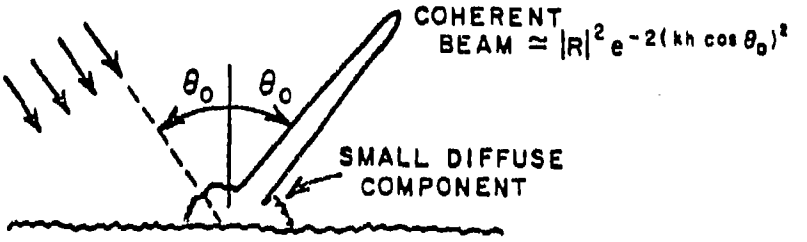

Figure 3.2-3. Scattering from a Slightly Rough Surface: $h \ll \lambda$, scattered beamwidth determined by transmitter beamwidth, predominantly coherent. (from [13])

and the height of the surface. Although the surface is random, it has a finite correlation distance, so that the scattering points are not independent.

Significant scattering power occurs in those directions which have significant Fourier components in the surface. This is usually known as Bragg scattering. In general, if the surface is composed of components, the scattering is proportional to those components which resonate with the vector difference between the propagation directions of the incident and scattered plane wave numbers.

For backscatter Barrick [14] gives the average normalized cross section for a slightly rough surface as:

$$\sigma^o = 4\pi k^4 \cos^4\theta_i \, |\alpha|^2 W\,(-2k\sin\theta_i, 0) \qquad (2)$$

where

$k = \frac{2\pi}{\lambda}$, is the RF wave number,

θ_i is the incidence angle (measured from the vertical),

α is a scattering coefficient which is a function of the surface materials, polarization states and incidence angle.

and

$W(\ell,m)$ is the two-dimensional Fourier transform of the two-dimensional autocorrelation function of the surface.

The scattering coefficient, α, for a nonmagnetic surface is:

$$\alpha_{hh} = \frac{\epsilon - 1}{(\cos\theta_i + \sqrt{\epsilon - \sin^2\theta_i})^2}$$

and

$$\alpha_{vv} = \frac{(\epsilon-1)[(\epsilon-1)\sin^2\theta_i + \epsilon]}{(\epsilon\cos\theta_i + \sqrt{\epsilon - \sin^2\theta_i})^2}$$

where ϵ is the relative permittivity of sea water. In the above expressions, "hh" and "vv" refer to horizontal and vertical polarization respectively. Table I gives ϵ as a function of frequency for a nominal water temperature of 10^o centigrade.

Table I. Complex Relative Permittivity of Sea Water at 10°C

Frequency GHz	Real Part	Imaginary Part
.5	83.6	-144.0
1.25	82.9	- 58.3
3.0	79.5	- 28.2
5.0	73.1	- 25.0
9.7	54.6	- 36.5
15.0	37.9	- 50.6
35.0	14.5	- 71.3

The general form of the sea cross section due to Bragg scattering has been known for some time. The greatest unknown in equation (2) is the magnitude of the sea surface spatial spectrum. Pierson and Stacy [5] give a detailed exposition of the spatial spectrum of the sea surface. They identify five regions of surface waves covering 6 orders of magnitude in wave number from wavelengths of 700 meters to .7 millimeters. Using available data from direct measurements of the sea surface, photographs of waves generated in wind-water tunnels, plus theoretical models, Pierson and Stacy generate a consistent quantitative model of the sea spectrum for each of the five regions. The resulting model is dependent only on the wind velocity over the sea surface.** Spectrums of the one dimensional spectrum from the model are given in Figure 3.2-4 and the various regions are marked.* On that figure, $U_{19.5}$ represents the wind speed measure at 19.5 m altitude, and $\bar{H}_{1/3}$ is the significant waveheight. Note from that figure, that at X and K_u band, the Bragg scattering will be influenced primarily by the capillary waves.

---

* Since we are concerned primarily with the capillary waves, only his region is discussed. The interested reader is referred to [5] for definitions and discussions of the 4 other regions.

** For a fully developed sea.

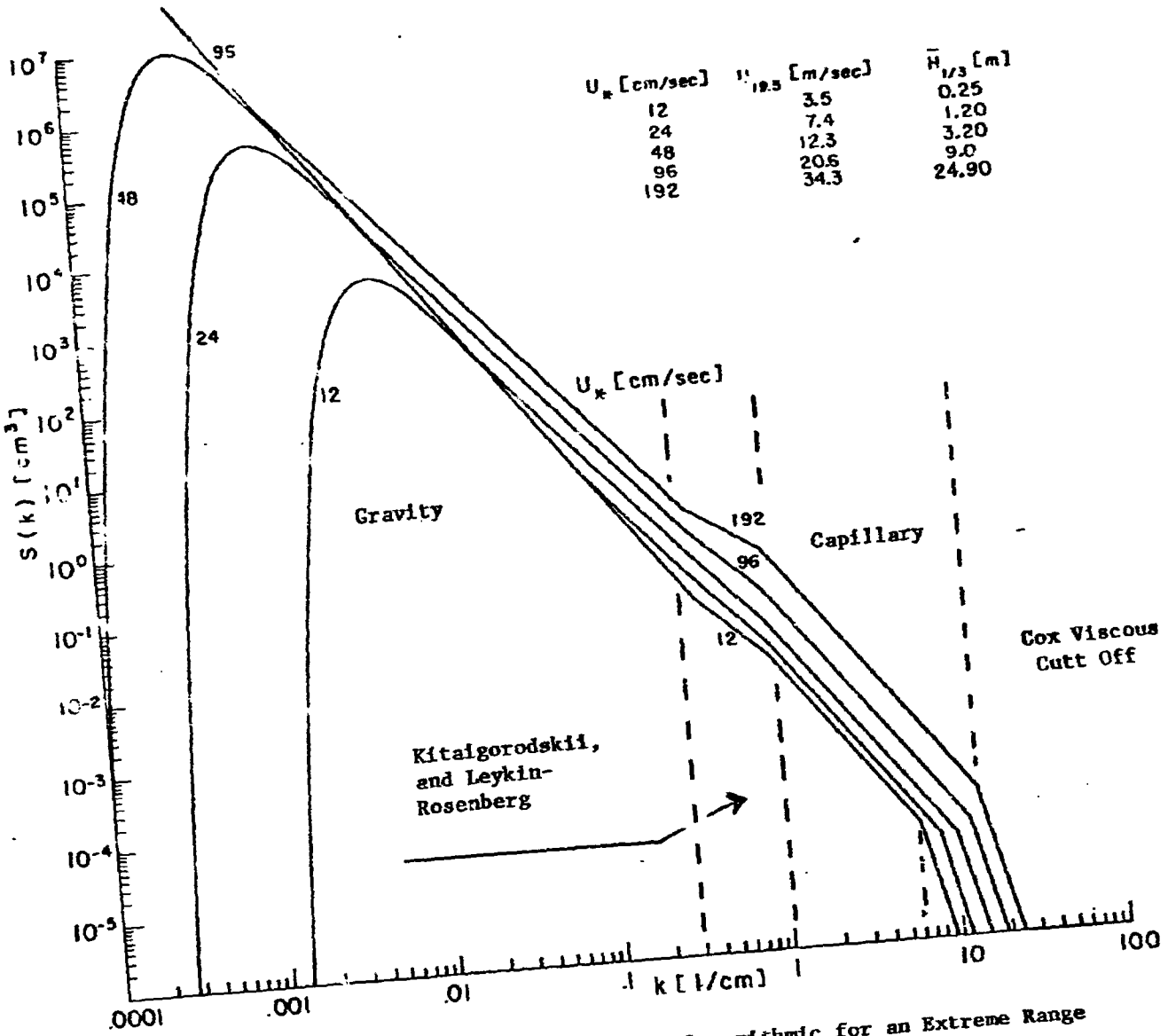

Figure 3.2-4. S(k) versus k with Both Scales Logarithmic for an Extreme Range of Wind Speeds. (from [5])

In the capillary region, Pierson and Stacy's model of the two dimensional wave spectrum is given as*

$$W_4(\ell,m) = \frac{.213\ H_c^2}{(\ell^2+m^2)^2}\ F(\ell,m) \qquad (3)$$

where

ℓ and m are the radar wave numbers in the upwind and cross wind direction.

H_c is the significant height of the capillary waves

and

$F(\ell,m)$ gives the anisotropy of the capillary wave spectrum.

In Pierson and Stacy's model, the capillary wave height is given as a rather complicated function. Figure 3.2-5 gives H_c versus wind speed.

Although it is relatively safe to extrapolate, the heights of the capillary waves from wind-water tunnels measurements to the open ocean, it is not possible to do so for the directional characteristics of the spectrum. The problem is that in a water-wind tunnel, the wind direction is very steady, and the resulting capillary waves tend to be generated at an angle to the wind direction as sketched in Figure 3.2-6. This results in a distinct bimodal, directionality to the wave spectrum. In the open ocean, the wind direction is constantly changing and tends to wash out the bimodal nature of the spectrum. For this reason, Pierson and Stacy were unable to determine a unique expression for $F(\ell,m)$.

To obtain a model for calculation, this author decided to use the direction coefficients inferred by Pierson and Stacy from some NASA upwind,

---

** In equation (3), the subscript 4 is for region 4 which is the capillary region. The reader should know that Barrick and Pierson differ by a factor of 2 in the definition of W. The relation is

$$W_{Barrick}(-\ell-m) = 2W_{Pierson}(\ell,m)$$

the expression given above is compatible with Barrick's definition so that it may be used in equation (2).

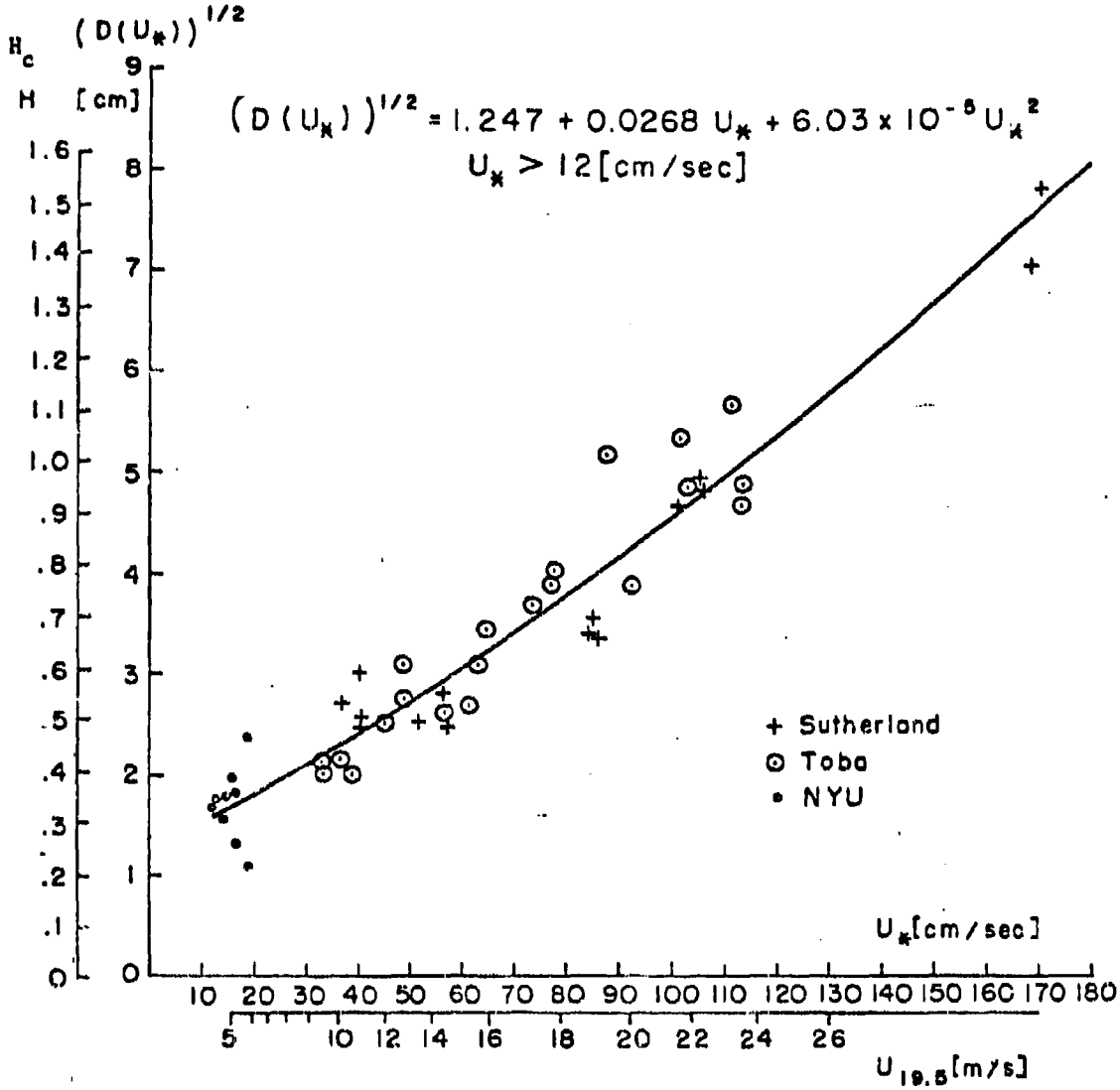

Figure 3.2-5. Capillary Waveheight Versus Wind Speed. $H_c \approx 0.195\,[D(U_*)]^{1/2}$ (from [5])

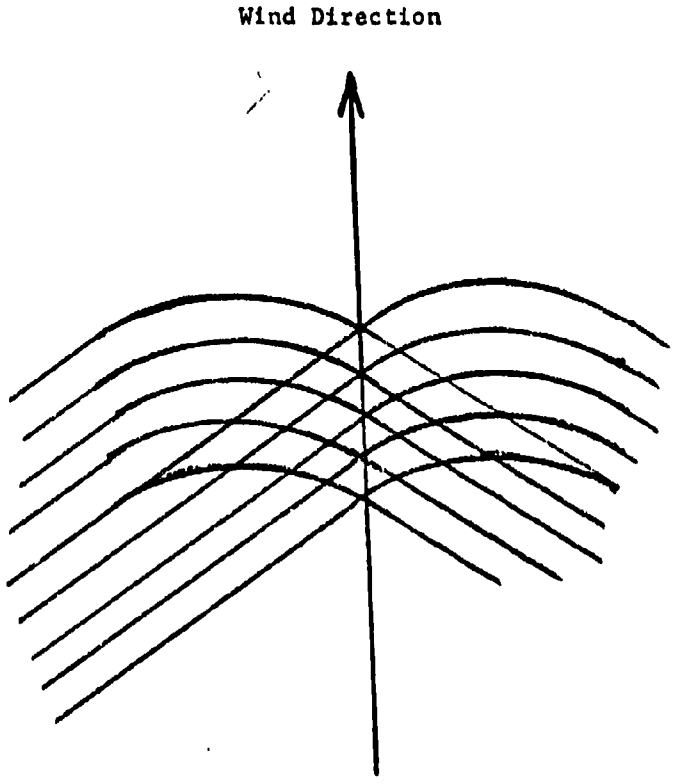

Figure 3.2-6. Sketch of Capillary Wave Patterns Produced by Steady Winds.

crosswind, radar measurements of relative σ^o at K_u band (Bradley [19]). Since these measurements were made over the open ocean, at a high enough frequency to insure capillary wave scattering, it was felt that they would be most suitable for comparison with the TAGSEA model. From these measurements, the directivity is given by

$$F(\ell,m) = F(\phi) = \frac{1}{\pi}\left[1 + a_1 \cos 2\phi\right] \tag{4}$$

where ϕ is the look direction relative to the wind direction,

and a_1 is a coefficient which depends only on wind speed.

That is,

$$a_1 = \frac{1.28\ U'^{.23} - 1}{1.28\ U'^{.23} + 1} \tag{5}$$

where

U is the wind speed at 19.5 meters height in knots.

Substituting (3) and (4), into the expression for backscatter (eq. (2)) yields:

$$\sigma^o = 0.167\ |\alpha|^2 (\cot^4 \theta_1)(H_c^2 F(\phi)) \tag{6}$$

Note in the above expression that the only term sensitive to RF frequency is $|\alpha|^2$. Table II gives $|\alpha|^2$ for horizontal and vertical polarization as a function of grazing angle and frequency. That table show negligible dependence on frequency; thus Bragg scattering from capillary waves is dependent only on polarization, grazing angle and wind velocity.

Equation (6) was evaluated for conditions comparable to the TAGSEA measurements and the results are given in Figs. 3.2-7 to 3.2-11. The comparison is good for vertical polarization cases. In those cases, the difference between the TAGSEA measurements and the theoretical model is about 1-2 dB. The comparison with the horizontal polarization measurements is not as good. The primary reason for this is that the model has not yet fully included the composite nature of the sea surface. In particular all the previous

Table II. Scattering Coefficients Versus Frequency and Incidence Angle, $|\alpha|^2$

		Incidence Angle						
Pol.	Freq.	20°	30°	40°	50°	60°	70°	80°
Hor.	C	0.655	0.677	0.708	0.748	0.798	0.857	0.925
	X	0.641	0.663	0.695	0.737	0.789	0.85	0.921
	K_u	0.655	0.677	0.708	0.749	0.798	0.857	0.925
	K_a	0.712	0.731	0.758	0.792	0.835	0.884	0.939
Vert.	C	0.991	1.66	3.25	7.5	21.1	80.5	560
	X	0.967	1.61	3.16	7.24	20.2	75.6	504
	K_u	0.992	1.66	3.25	7.47	20.9	78.6	524
	K_a	1.09	1.83	3.62	8.45	24.1	94.4	675

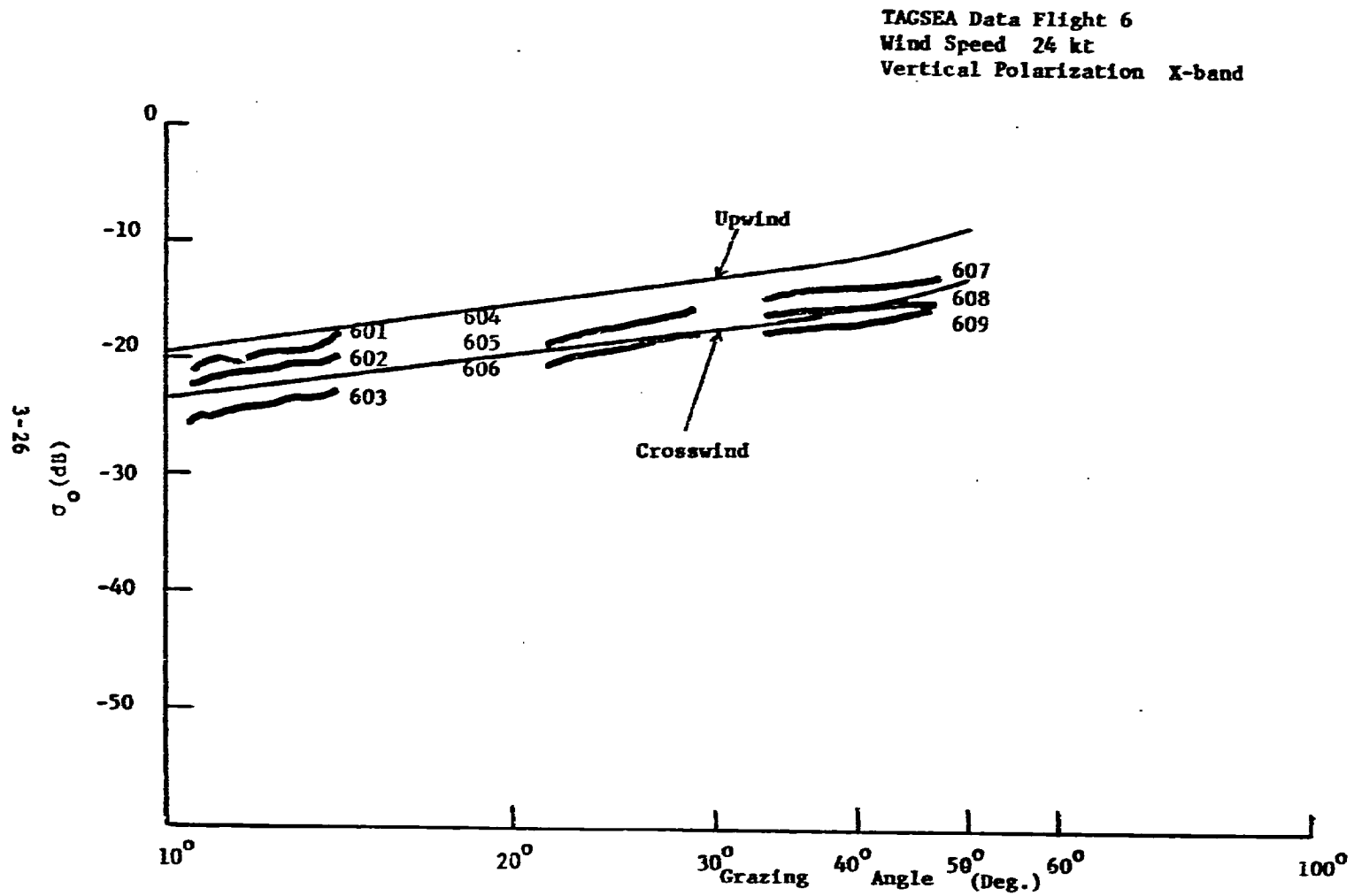

Figure 3.2-7. Comparison of TAGSEA Data with Equation (6).

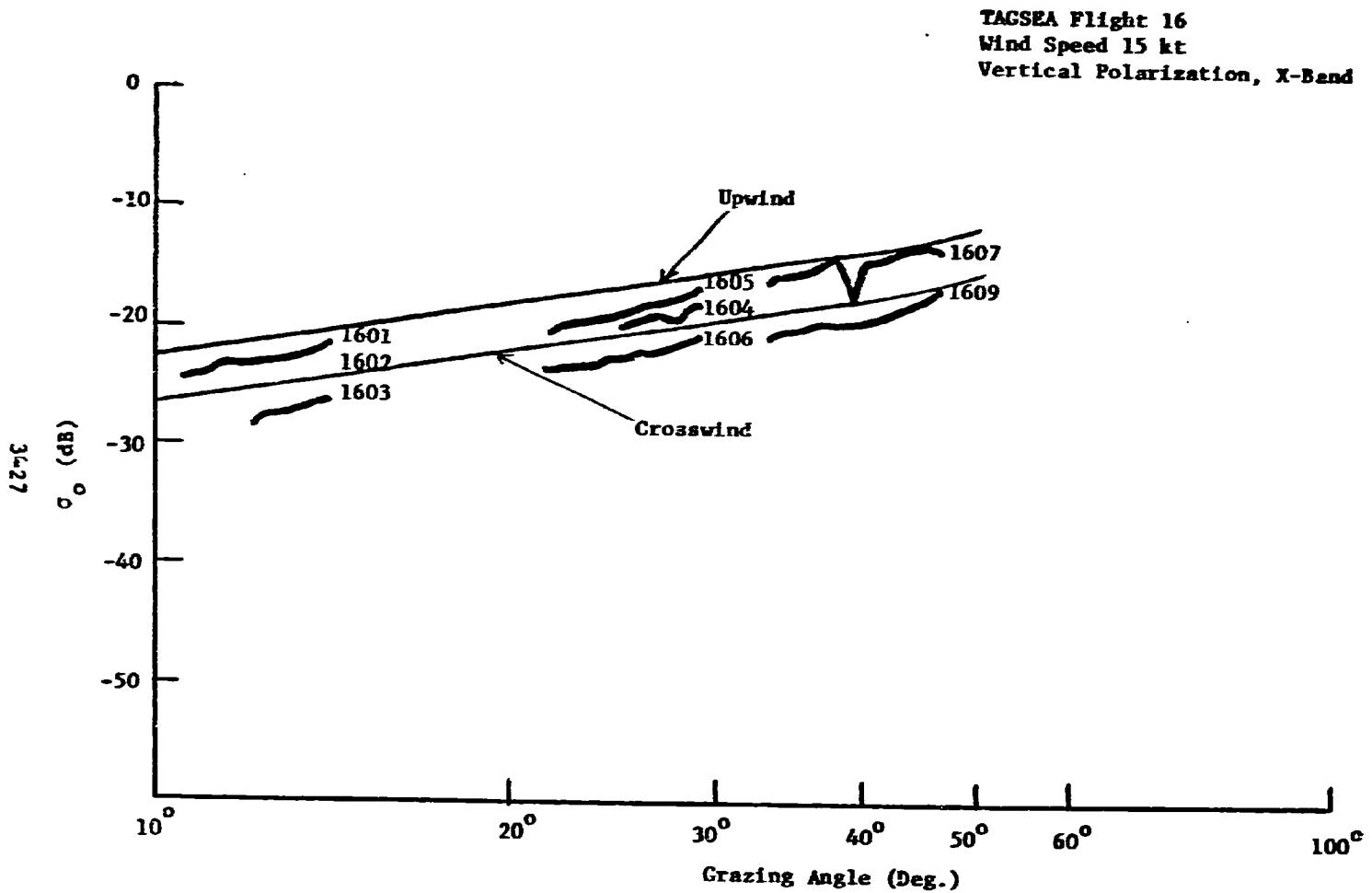

Figure 3.2-8. Comparison of TAGSEA Data with Eq. (6).

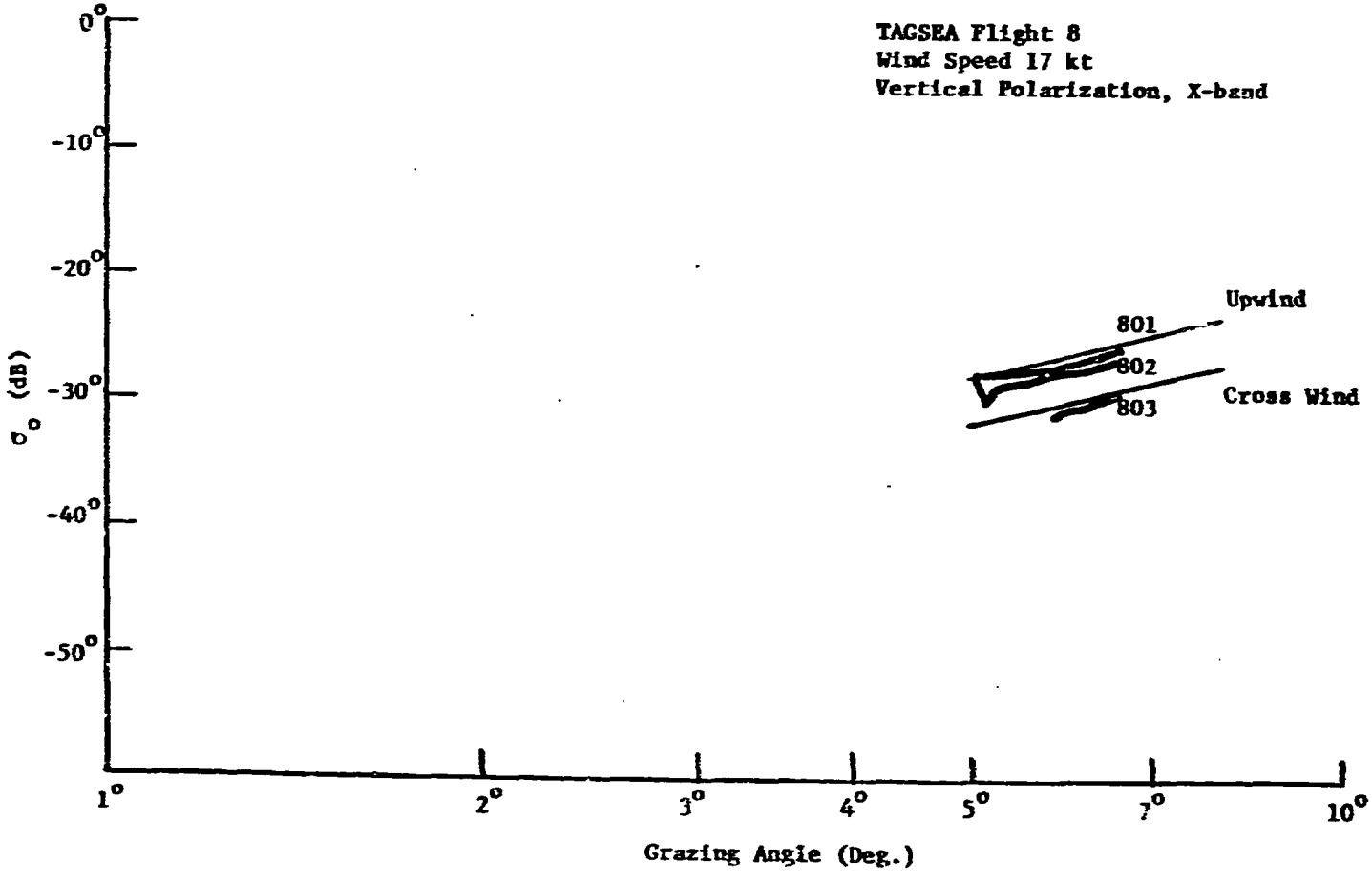

Figure 3.2-9. Comparison of TACSEA Data with Equation (6).

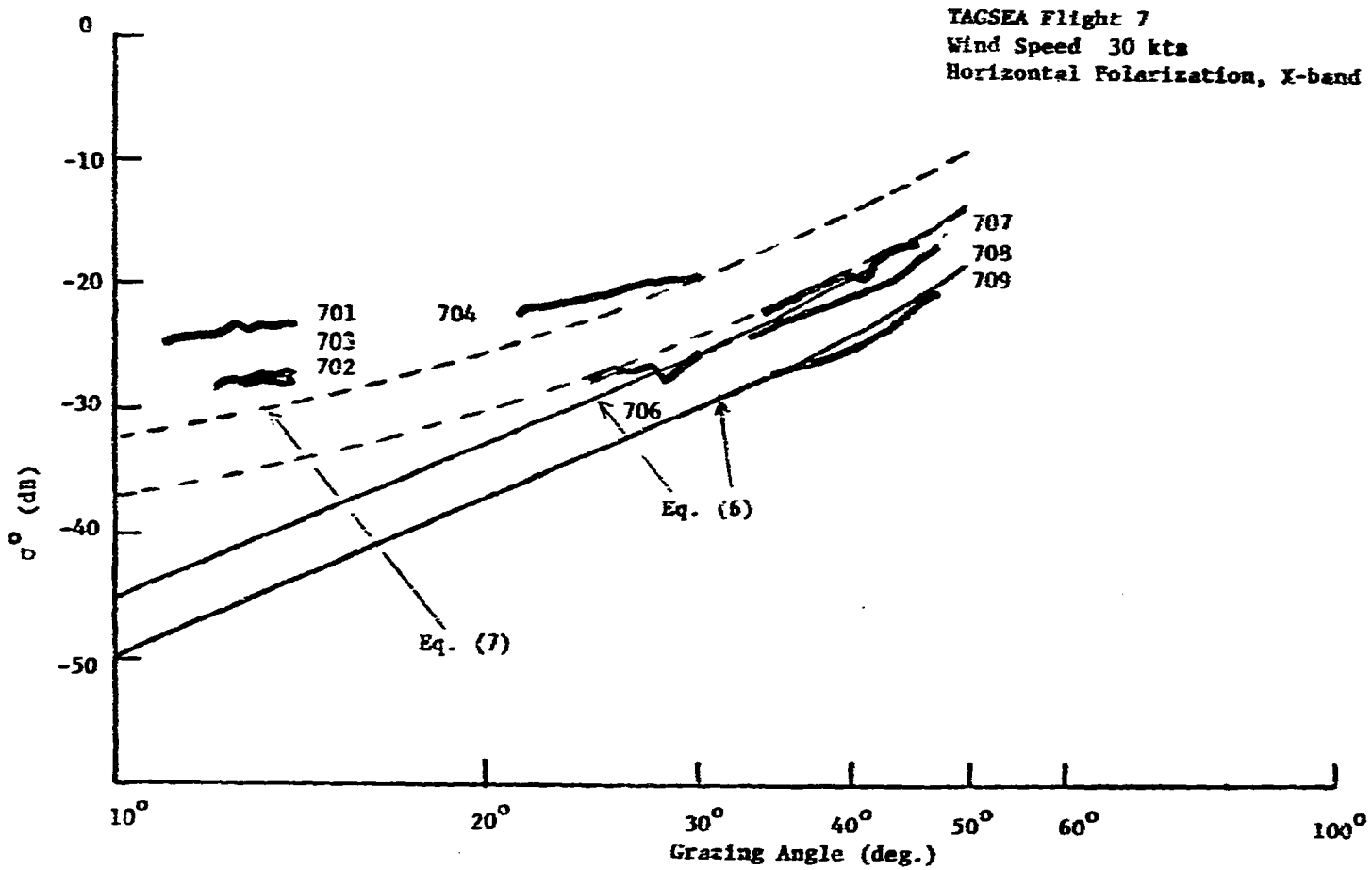

Figure 3.2-10. Comparison of TAGSEA Data with Eqs. (6) and (7).

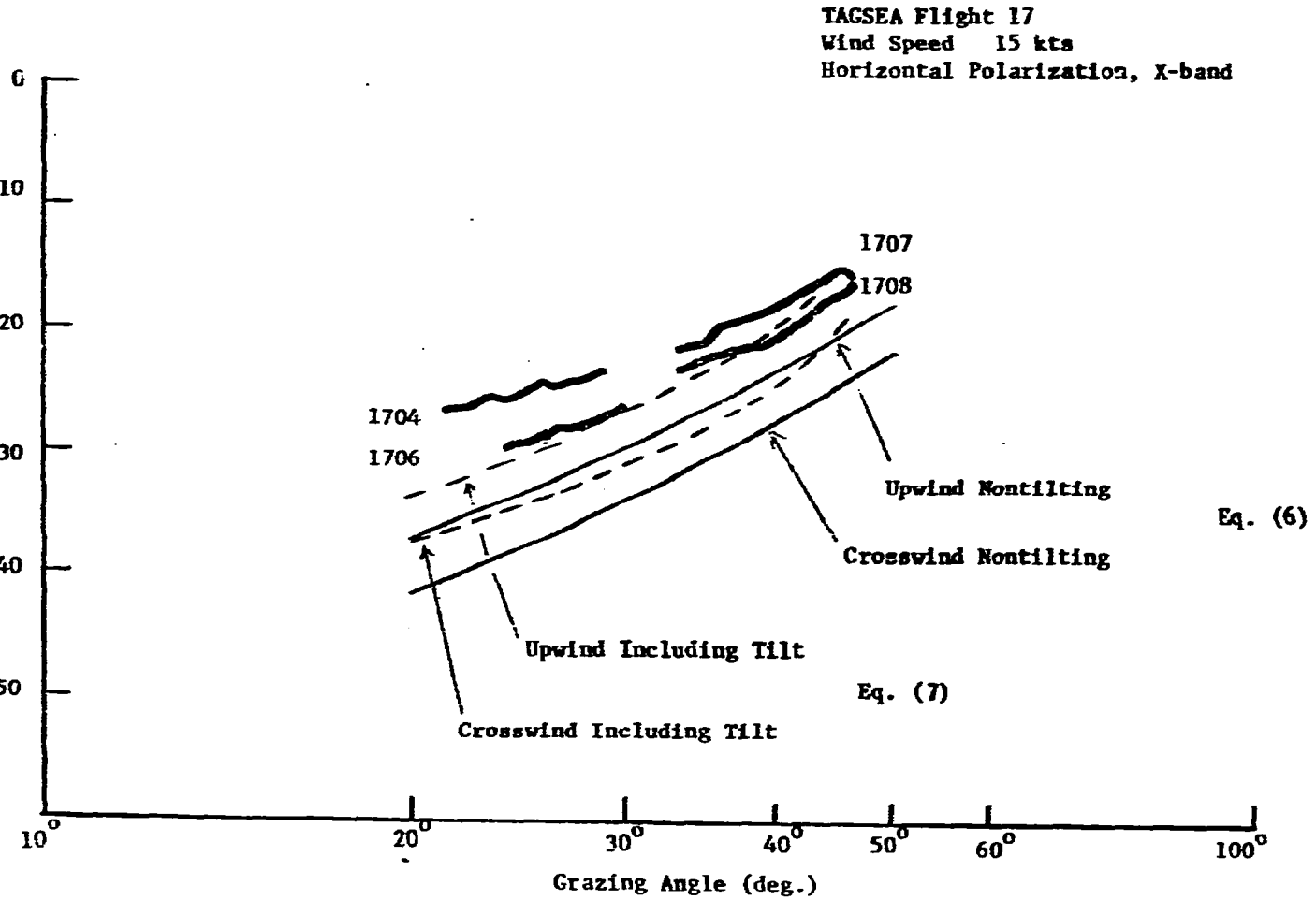

Figure 3.2-11. Comparison of TAGSEA Data with Eq.s (6) and (7).

derivations were made for a slightly rough; flat, horizontal surface. In fact, the capillary waves are superimposed on a larger gravity wave structure, as sketched in Figure 3.2-12

At sea state 5, the gravity wavelength is on the order of 60-80 meters; thus for the short TAGSEA resolution cell ($\approx$ 30 m), the portion of the gravity wave seen is fairly flat, but it is not horizontal. Instead as each wave passes through the range cell, the local angle of incidence varies according to the slope of the wave. To obtain the average cross sections, the cross section computed from eq. (6) must be averaged over the variations in the angle of incidence produced by the gravity waves. If P(S) is the probability density distribution of the wave slopes, the average cross section is given by:

$$\overline{\sigma_o}(\theta_i) = \int_0^\infty \sigma_o(\theta_i - \tan^{-1}(S))\ P(S)\ dS \qquad (7)$$

The above computation will have little effect on the mean cross section for vertical polarization since σ^o_{vv} varies slowly with incidence angle. However, it will have a significant effect on the horizontal polarization results.

Eq. (7) was evaluated for horizontal polarization assuming a Gaussian slope distribution with an rms slope gain be eq. (1a). The results are plotted as dotted lines in Figures 3.2-10 and 3.2-11. Note that the agreement is better, but still not as good as the vertical polarization results. The reasons for this are not known. One possibility is the horizontal tilting of the gravity waves. That is, in addition to tilting "fore and aft", the gravity waves also tilt "side-to-side". When the surface is tilted side-to-side, the incident electric field is no longer exactly horizontally polarized with respect to the local surface tilt. Thus, locally, the wave has slight vertical polarization. Since vertically polarized backscatter at low grazing angle is 10-15 dB higher than horizontal polarization, a slight "local vertical" component will significantly change the σ^o characteristic. Unfortunately the computations required to do the two dimensional averaging were too tedious to complete for this report. It should be noted that in his model, Wright [24] did include tilting in both directions. He also was able to obtain good agreement for vertical polarization but stated that the horizontal polarization results were not as good. There are several differences in the details between the model used here, and Wright's model, but the primary difference is in the assumed water-wave spectrum.

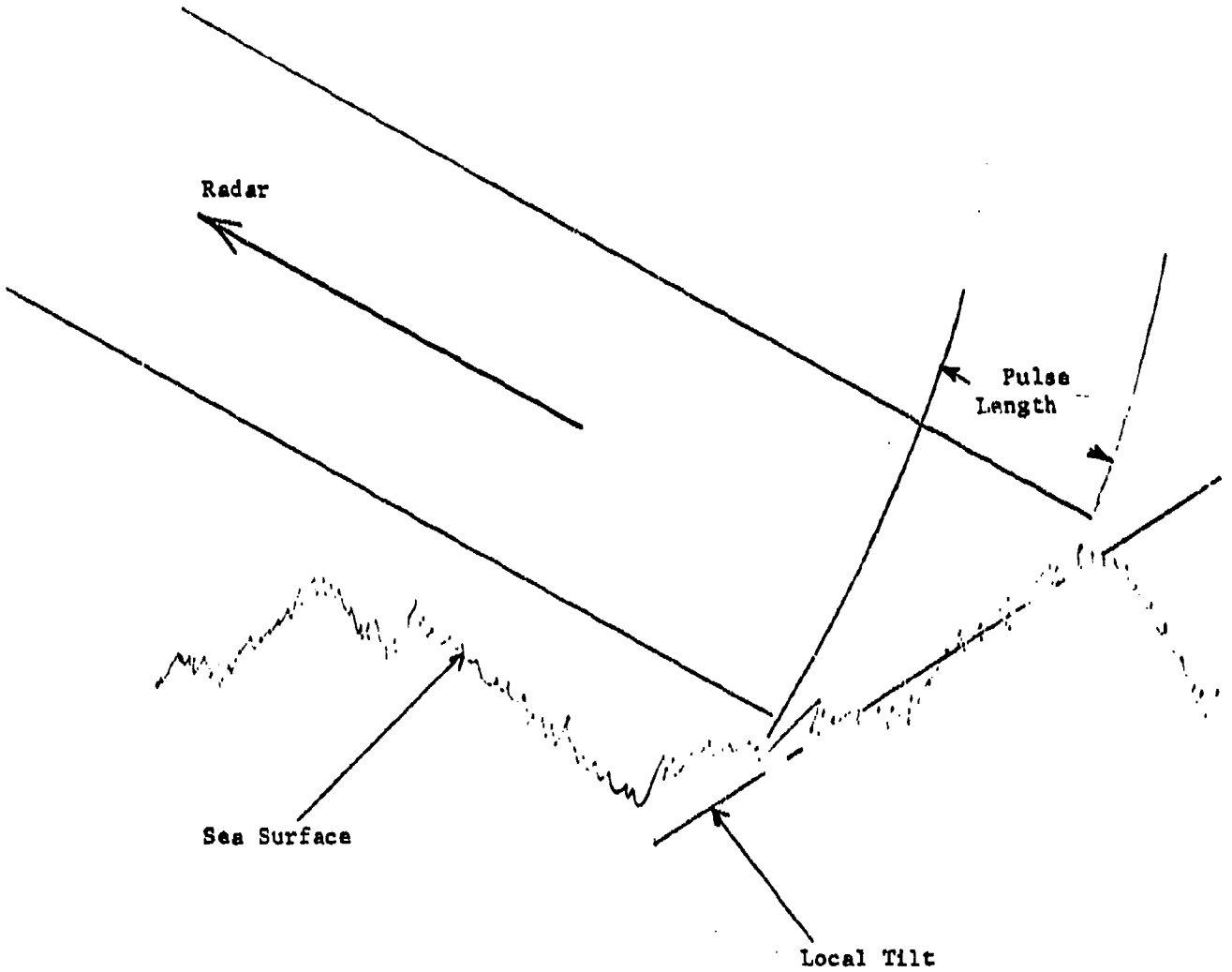

Figure 3.2-12. Local Tilting of the Surface due to Large Scale Gravity Waves

The results indicated in Figures 3.2-7 to 3.2-11 are encouraging and indicate that the Bragg scattering model superimposed on a tilting surface as described above compare favorably to the TAGSEA measurements. Further, Pierson and Stacy's model was derived by a compltely independent procedure, the favorable comparison to the TAGSEA results tends to validate both sources.

It should be noted that Pierson and Stacy compared their model to NRL backscatter measurements. They were able to get very good agreement except for a factor of about 12 or 4π bias between their predicted backscatter based on their model, and NRL measurements. They implied that the NRL measurements were too low by a factor of 12. Since NRL data represents the most comprehensive set of clutter measurements, all TSC clutter models published previously have been heavily biased by the NRL data.

3.2.2 Implications of the Theoretical Model on the Statistical Fluctuation of Sea Backscatter

The model discussed above leads fairly naturally to a space and time varying Rayleigh fluctuation model as proposed by several authors (e.g., Guinard and Daley [20], Sodergren [8], Tong [21], and Trunk [22]). The instantaneous measured cross section consists of a short term fluctuation which is determined by the scattering from the capillary waves. The mean level of this short term scattering is given by eq. (6). Note that the expression depends on the local angle of incidence and the mean wind velocity. As different parts of sea are examined, the local angle of incidence will vary as the gravity waves and swell cause tilting of the surface. Further, spatial variations in wind velocity (turbulence) cause the height of the capillary waves to vary accordingly. As noted by Pierson and Stacy [5], the capillary waves build up very quickly and act as almost instantaneous tracers of the local wind speed.

Qualitatively, such a model compares favorably with the TAGSEA model proposal in [1]. In that reference, the fast fluctuation component was assumed independent from FFT frame to FFT frame. Thus in that model, the fast component decorrelates in 9 milliseconds or less. The slow fluctuation component was modeled as having a spatial correlation of 300 to 1000 feet and a temporal correlation of 3 to 10 seconds.

Quantitative comparisons between a theoretical model based on Bragg scattering and Pierson and Stacy's sea surface model are difficult to make. Generally very careful interpretation of the sea surface model and its interaction with the radar system is required to obtain a good quantitive estimate. Further, formulas resulting from the model usually require fairly involved numerical evaluations. For these reasons, no attempt to make detailed computations will be made; however, some relatively quick calculations can be considered.

An estimate of the rate of fluctuation for the fast component can be obtained by considering the "phased array" model for the diffuse component as discussed earlier. At any instant of time the diffuse spatial scattering appears as random sidelobes, produced by the random phase errors, caused by the capillary waves on the surface as depicted in Fig. 3.2-13.

The scattering pattern will change as the structure of the capillary waves changes. In addition as the aircraft flies along it samples the scattering pattern in space at an angular rate:

$$\dot{\Omega} = \frac{V}{R} \tag{8}$$

For a given resolution cell size, the average angular width of a lobe in the scattering pattern can be expected to be

$$\bar{\Omega} = \frac{\lambda}{D} \tag{9}$$

Thus if the surface is "frozen" and the main effect is the aircraft motion through the scattering pattern, the correlation time is approximately:

$$\tau = \frac{\bar{\Omega}}{\dot{\Omega}} = \frac{\lambda R}{DV} \tag{10}$$

For D=30m, R=1500m, λ=.03m, V=130m, the correlation time is:

$$\tau = .011 \text{ sec.}$$

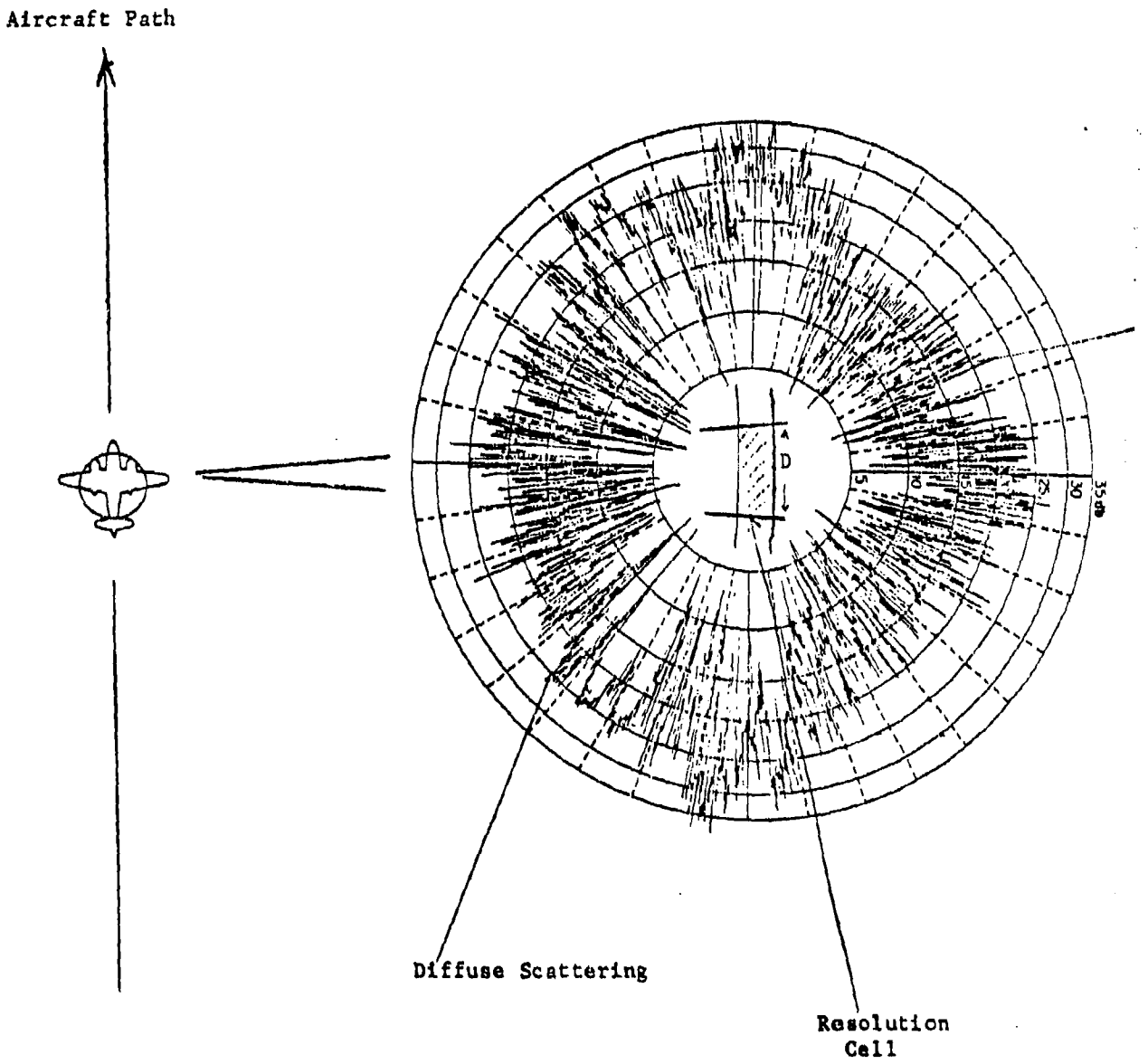

Figure 3.2-13. Rapid Fluctuation of Scattering Caused by Aircraft Motion

For this case, the fast fluctuation component decorrelates sample-to-sample in agreement with the TAGSEA model. Note that this relation will always hold if the azimuth resolution is obtained by synthetic aperture techniques. However, if the A/C were flying towards the resolution cell, the significant angular rate would be in the vertical plane, and would be

$$\dot{\Omega} = \frac{V \sin \varphi}{R} \tag{11}$$

where φ is the grazing angle. Continuing the example, the aircraft's contribution to correlation time is

$$\tau = \frac{\lambda R}{D V \sin \psi} = .06 \text{ sec. maximum*}$$

at 10° grazing angle. Thus for the forward looking cases, the correlation time of the fast fluctuating component might be significantly longer than for the sidelooking case if it were not for wave motion. Note that the theoretical model would indicate that in nonsynthetic aperture cases and for high processing frame rates, the fast fluctuation component would be correlated. The TAGSEA model implies (but does not state specifically) that the fast fluctuating component is independent under all conditions.

The theoretical model can also be used to approximate the characteristics of the slowly fluctuating component. Recall from eq. (6) that the mean cross section is a function of local wind speed and local grazing angle. Using Pierson and Stacy's [5] model for gravity waves it is possible to approximate the variation in local grazing angle. Further, using models of atmospheric turbulence (e.g., Kalbaugh [23]), it is possible to approximate the variations expected due to these variations in local wind conditions. As noted earlier, detailed computations will not be attempted here. However, it is interesting to note that if the rms variation in the cross section is computed using Eq. (6) and averaged over a Gaussian slope distribution, the values are close to 0.2 as shown in Table III for a typical case. This value corresponds to the extreme mean variation case noted in the TAGSEA model.

A final comparison between the TAGSEA model and the theoretical model is in the underlying distribution for the rapidly varying component. The TAGSEA model proposes a slightly nonrayleigh distribution to model the rapidly fluctuating component. From the previous discussion, it might be

---

* NOTE: This ignores the wave dynamics of the sea.

Table III. RMS Variation in the Long Term Fluctuation
(Theoretical Computation)

- o Wind Velocity 15 kt
- o Vertical Polarization

Grazing Angle (deg.)	RMS Variation (dimensionless)
10	.57
20	.28
30	.21
40	.23
50	.33

inferred that the theoretical model would imply a Rayleigh distribution for the rapid fluctuations. It should be noted that the Bragg scattering model is not a many, equal, independent scatterer model. The received field is modeled as the spatial Fourier transform of the capillary wave heights over the illuminated range-azimuth resolution cell. In a mathematical sense, the Fourier transform will be Gaussian (Rayleigh amplitude) only when the capillary waves can be represented as a stationary Gaussian process. As a practical matter, the exact distribution of the capillary waves is not as important as the assumption of stationarity. As noted above, gravity waves and swell can produce significant nonstationarity by tilting the local surface. It is reasonable to ask under what conditions will the sampled σ^o fluctuations approximate a Rayleigh (power) distribution.

Two extreme cases are of interest. In the first extrema, the resolution cell is so broad that the tilt and gusts are averaged out and the residual σ_o variations are negligible. This is the usual low resolution radar limit. At the other extreme, the resolution cell is kept fixed relative to the surface, and the samples are taken in so short a time that the sea surface and wind gusts are "frozen". By sampling the resolution cell from different aspects, one can obtain independent samples from the Rayleigh distribution which correspond to that cell. Note however, that the maximum number of samples which can be obtained is limited. In the TAGSEA case, it was shown earlier that the maximum independent sampling rate is about .011 sec. For a resolution cell of size 30 m, the dominant tilting effect is from gravity waves of approximately the same size. Thus, the tilting should occur with a nominal frequency of

$$\frac{\omega}{2\pi} = \frac{\sqrt{gk}}{2\pi} = .22 \text{ Hz.}$$

The available number of samples is on the order of 400, and it is difficult to obtain accurate statistics from such a limited sample size. One possible approach would be to normalize the statistics to the mean level of the 400 samples, and then cumulate statistics on the normalized data. The result should approach a Rayleigh distribution. It should be noted that the above procedure does not correspond to the N-type normalization used in reference [1].

Although the data was normalized by range gate and over short time periods, it should be noted that for histogram analysis, all Doppler bins were cumulated without normalization. The total Doppler spread corresponds to approximately 3200 feet along the aircraft track; thus the data is taken such that several different gravity wave systems are lumped together. The result is that the N-type fast fluctuations seen by the TAGSEA data analysis correspond to a non-Rayleigh distribution.

It is quite likely that the differences mentioned above are largely academic since most CFAR systems average over several range cells, and often over several azimuth cells. Thus the distribution seen by the CFAR circuit will be non-Rayleigh as proposed by the TAGSEA model.

In summary, the TAGSEA model agrees well qualitatively with a time and space varying Rayleigh distribution. The theoretical model is based on a composite sea surface model for which the dominate scattering mechanism is Bragg scattering from the capillary waves. Gravity waves and swell serve to introduce nonstationarity into the data by tilting the local surface in a resolution cell. Additionally, preliminary calculations indicate significant quantitative agreement exists between the theoretical model and the TAGSEA data for vertically polarized cases. Since the sea surface spectrum proposed by Pierson and Stacy [5] is based on direct water-wave measurements rather than radar measurements, the quantitative agreement tends to lend credence to both results. Quantitative results for horizontal polarization are not as good at least for reflectivity.

3.2.3 Comparison of the TAGSEA Fluctuation Model with Other Published Results

Although there are several sources for published results on the average sea clutter cross section, there are fewer published results on the fluctuation statistics of σ_o. Most investigators consider only the composite distribution (Type-A or second order model in the nomenclature of [1]). In a following subsection, the TAGSEA model for "Type-A" distributions will be compared to several other experimental results.

To this writer's knowledge, four authors ([24], [22], [21], and [8]) give detailed characteristics of a model which attempts to describe the underlying long term fluctuation characteristics as was done in the TAGSEA third order model.

Wright [24] considers only the mean cross section as was done in the previous section. He obtained comparable results in that his results for vertical polarization agree well with backscatter data. Trunk [22] computed the statistics of the composite distribution using nearly the same formulas as were given in the previous section. He also averaged results over a one dimensional slope distribution, but based his calculations on the Kitaigorodskii model of the water-wave spatial spectrum* Trunk's results for vertical polarization were compared to the TAGSEA model in reference [1]. There it was shown that Trunk's results compare well with the TAGSEA data.

Tong [21] indirectly inferred the characteristics of the underlying distribution by matching theoretical calculations to observed statistical distribution functions.

Sodergren [8] presents experimental results on both the composite distribution (That is, the distribution which reflects both the long and short term trends.) as well as giving characteristics of the long term fluctuations. Since theoretical calculations were presented previously, only Sodergren's data will be compared to the slow fluctuation characteristics of the TAGSEA third order model.

3.2.3.1 Comparison to Experimentally Measured Composite (Type-A) Distributions

In this subsection, the TAGSEA model is compared to the σ_o fluctuation statistics measured by other experimenters. The data to be compared corresponds to the TAGSEA second order model, that is, the composite distribution arising from both the long term and the short term fluctuations.

Although several references are available for obtaining the fluctuation statistics, most references are not directly comparable to the TAGSEA measurements. In particular, Brooks and Brooks [25] show that the

* See Pierson and Stacy [5] or Trunk [22] for a description of the Kitaigorodskii water wave spectrum.

published references exhibit a moderately strong trend of increasing skewness in the composite distribution versus grazing angle. Figure 3.2-14 taken from [25] shows that below about 8 or 9 degrees grazing angle, the ratio of the 84 percentile to the 50 percentile increases as $\sin^{-1}\psi$. Thus data taken at low grazing angles should exhibit significantly higher tails than the TAGSEA data which was taken at grazing angles of 5° and greater. This is demonstrated in Tables IV, V, and VI. In those tables, the TAGSEA model is compared with data taken by Bishop [10] and Rivers [11]. Both sets of data were taken at low grazing angles in shallow water. On Figure 3.2-14, Bishop's data yields high values of σ' (7-17 dB) and as seen from Tables V and VI, the distributions lie significantly above the TAGSEA model. Rivers data on the other hand generates relatively low values of σ' (4-6 dB) but still lies significantly above the TAGSEA model.

The above comparisons, obviously, provide no information on the validity of the TAGSEA model. They do, however, serve to emphasize the limitations of the model as stated in [1]. The model was derived to apply only to the conditions for which the greatest amount of data was available. Thus the TAGSEA model applies only to moderate grazing angles (5°-45°), high sea state (4-5), and deep water data. As the above comparisons indicate, conditions which deviate significantly from the TAGSEA experiment are likely to require significantly different models. As reference [25] indicates, the greatest effect may be grazing angle.

A review of the available references indicates that references [6]-[9] and [26], [27] have data for grazing angles above 5 degrees. From this data base, results based on the NRL four frequency radar must be eliminated since that radar is a low resolution radar. Although the pulse length is reasonably small for that radar, the beamwidth is quite wide ($\approx 5^{\circ}$) and the azimuth resolution cell is broad. Upon inspection of the references, it was found that many of the references presented the same data. Thus after eliminating the redundancy, it was found that only Trunk and George [6], Schmidt [7], Sodergren [8], and Boeing [9] represent nonredundant, high-resolution, moderate-grazing angle data for comparison with the TAGSEA model.

Figure 3.2-14. σ'_{dB} Versus Grazing Angle

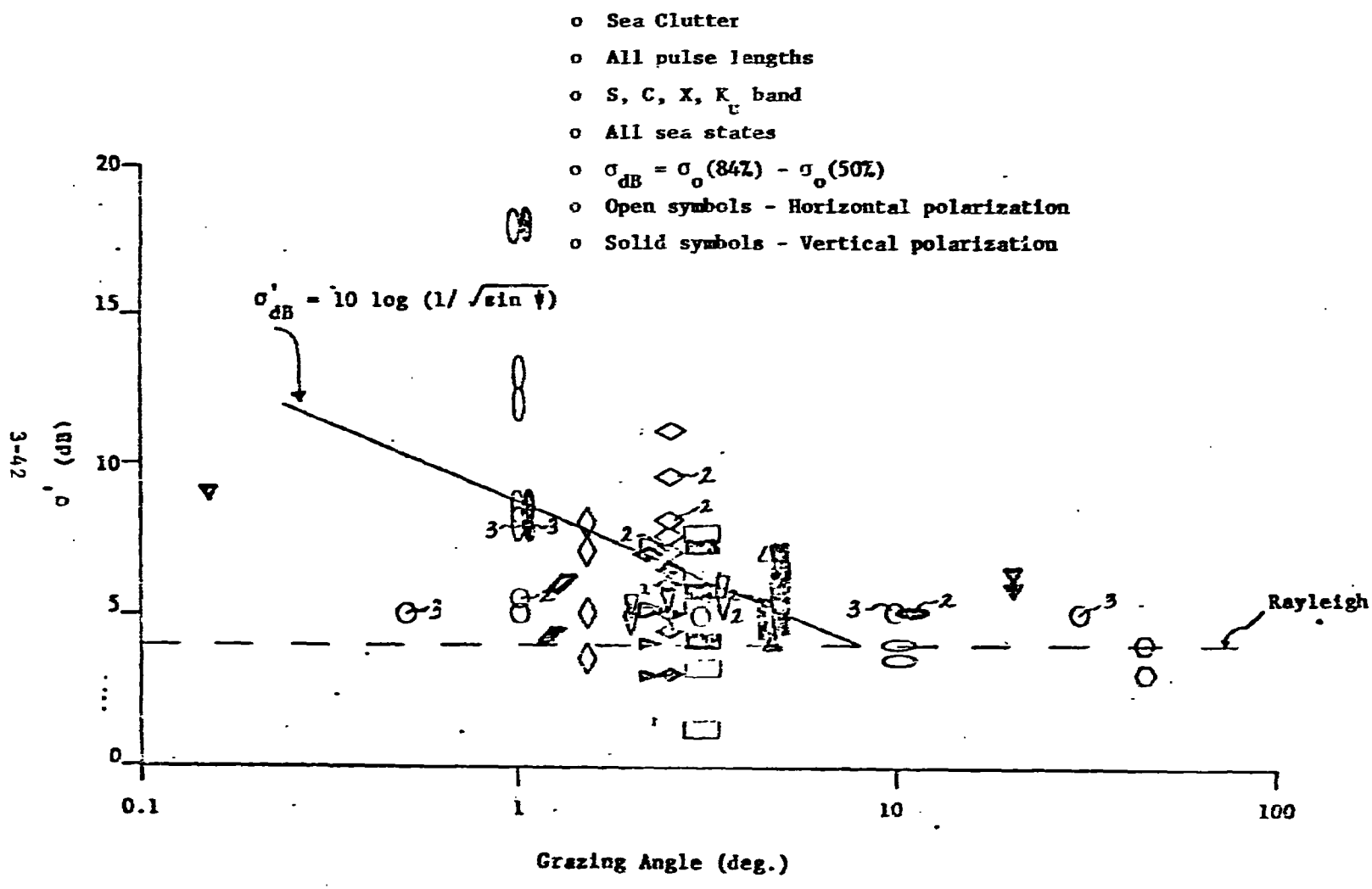

Table IV. Comparison of the TAGSEA Model with Bishop [10]

- o Vertical Polarization
- o Level in dB re mean
- o Bishop data at 1^{o} grazing
  45 x 40 m

Prob. of Exceed.	TAGSEA Typical	TAGSEA Extreme	Bishop Data			
			SS-4-5	SS-2-3	SS-3	SS-6
10^{-1}	3.6	3.6	4.0	4.5	4.0	4.5
10^{-2}	7.1	7.0	9.0	10.0	9.0	10.5
10^{-3}	9.3	9.4	11.5	13.0	13.6	15.5
10^{-4}	10.9	11.5	13.8	14.6	16.7	19.7
10^{-5}	12.2	13.4	15.0	16.0	19.5	21.3
10^{-6}	13.3	15.2				

Table V. Comparison of TAGSEA Model with Bishop [10]

- o Horizontal Polarization
- o Level in dB re mean
- o Bishop at 1° Grazing, 45 x 40 m

Prob. of Exceed.	TAGSEA Typical	TAGSEA Extreme	Bishop Data			
			SS-5	SS-3-4	SS-2	SS-1-2
10^{-1}	3.5	3.4	4.0	4.0	4.0	4.0
10^{-2}	7.6	8.1	10.0	10.0	12.0	12.0
10^{-3}	10.4	11.6	12.2	13.6	15.6	19.6
10^{-4}	12.6	14.5	13.8	15.8	18.2	21.2
10^{-5}	14.6	17.1	15.0	17.6	19.0	22.0
10^{-6}	16.4	18.5				

Table VI. Comparison of the TAGSEA Model with Rivers [11]

- o Grazing Angle ≈ 1.5°
- o Echo Area ≈ 12 m x 30 m
- o Level in dB re mean
- o Wind Speed 9.5 kts (SS 3)
- o X-band, Upwind

Prob. of Exceed.	Horizontal Polarization			Vertical Polarization		
	TAGSEA Typical	TAGSEA Extreme	Rivers	TAGSEA Typical	TAGSEA Extreme	Rivers
10^{-1}	3.5	3.4	3.6	3.6	3.6	3.8
10^{-2}	7.6	8.1	9.8	7.1	7.0	7.8
10^{-3}	10.4	11.6	14.6	9.3	9.4	11.1
10^{-4}	12.6	14.5	19.1	10.9	11.5	14.0
10^{-5}	14.6	17.1		12.2	13.4	
10^{-6}	16.4	18.5		13.3	15.2	

The characteristics of the data which can be compared to the TAGSEA data are given in Table VII. Of these references, Sodergren's results were already compared with the TAGSEA data in [1]. As can be seen from Figure 3.2-15 taken from [1], his results compare well with the TAGSEA second order model. A more complete discussion of Sodergren's model versus the TAGSEA model is given later.

The Boeing results are preliminary, have only been reported informally, and are at S-band. For these reasons, it would be premature to report on them in detail. However they did observe non-Rayleigh distributions. When they fit the linear envelope with a Weibull distribution they obtained an, "N" parameter of ≈1.75. This result is not inconsistent with the TAGSEA results which obtained a Weibull parameter of ≈.8 for the square law detected output [4].* A linear law Weibull parameter of 1.75 corresponds to a square law Weibull parameter of 1.75/2 = .875.

Table VIII compares distributions given by Trunk and George [6] and Schmidt [7] with the TAGSEA model. As can be seen, the data in Table VIII appears to be significantly higher than the TAGSEA model. Trunk and George's results appear to be quite high, and in fact may have been selected for that reason since they were reported in an introduction to a paper on detection in nongaussian clutter. Another possibility is that the extremely short pulse length (3 m) of that data may contribute to the high tails. Schmidt's data, taken at higher sea state with the same radar does not have as high tails as the data presented by Trunk and George. Note that Schmidt's data contradicts

---

* The approximate value for N corresponding to the Weibull distribution can be obtained from the statistical parameters given in Section 1.2 of ref. [4]. For a given value of Q, the percentile, X, corresponding to that value is given by:

$$X = \frac{\mu(-\ln Q)^{1/N}}{\Gamma(1 + N^{-1})}$$

where N is the Weibull parameter, μ is the mean, and Γ is the gamma function. In Section 1.2 of [4], the data is normalized so that μ=10. Thus for N=.8 and Q=10^{-5}, then X=22.7 dB. This corresponds to row #14 of the table given in Section 1.2.1 of [4], in that reference the values vary from about 21.5 dB to 28 dB.

Table VII. Data Compared to the TAGSEA Model

Reference	Grazing Angle	State Sea	Polarization	Resolution	Freq.	Look Direction
Trunk and George [6]	4.7°	1-3	V	40 x 3 m	X	D?
Schmidt [7]	4.7°	5-6	V,H	40 x 3 m	X	U
Sodergren [8]	.5°-40°	2-4	H	30 x 15m	X	U,D
Boeing [9]	4.5°	3,6	H	? x 40m	S	C,D,U

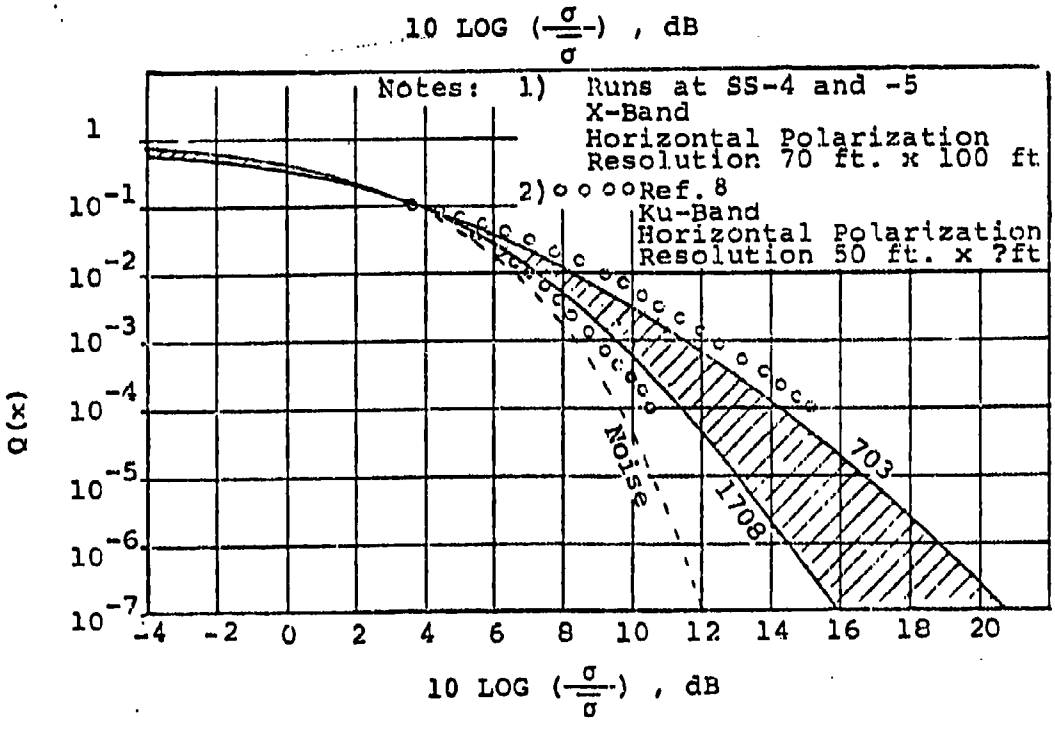

Figure 3.2-15. Comparison of the TAGSEA Composite Distribution to Sodergren's Data [8].

Table VIII. Comparison of the TAGSEA Model with Trunk and George [6] and Schmidt [7]

	Vertical Polarization					Horizontal Polarization		
Prob. of Exceed.	TAGSEA Typical	TAGSEA Extreme	Trunk & George [6] SS-1	Trunk & George [6] SS-2-3	Schmidt [7] SS-5-6	TAGSEA Typical	TAGSEA Extreme	Schmidt [7] SS-5-6
10^{-1}	3.6	3.6	4.4	4.7	3.5	3.5	3.4	3.1
10^{-2}	7.1	7.0	9.1	10.3	8.5	7.6	8.1	10.1
10^{-3}	9.3	9.4	11.8	14.1	11.5	10.4	11.6	14.1
10^{-4}	10.9	11.5	12.6	16.8		12.6	14.5	
10^{-5}	12.2	13.4				14.6	17.1	
10^{-6}	13.3	15.2				16.4	18.5	

Trunk and George's data which shows higher tails at higher sea states. Further, the trend of higher tails at higher sea states is not completely consistent with Bishop's vertical polarization data (Table IV). However Bishop also shows atypical cases which contradict his trend of lower tails with higher sea state.

It does not appear possible to prove or disprove the validity of the TAGSEA model on the basis of other experimental data. It is possible to find data which agrees and data which disagrees with the model. When the rather large list of references which give distribution functions is sifted to obtain those data which can be directly compared to the TAGSEA model, it is found that only four data sets are left. Of these data, Sodergren's data and the Boeing data have the strongest similarity to the TAGSEA model. The other data, taken by the NRL 20 nsec radar have higher tails for the composite distribution. Thus it would appear to be a conservative design practice to at least consider the effect on system performance of tails which are 2-3 dB higher at the 10^{-4} point on the distribution.

3.2.3.2 Comparison with Sodergren's Fluctuation Model

As noted earlier, Sodergren is the only source for an experimentally determined model comparable to the TAGSEA third order model. As has been noted, Sodergren's distribution functions compare favorably with the TAGSEA second order model. In this section, comparisons related specifically to the third order models will be made.

Sodergren, TAGSEA and several theoretical models propose a composite fluctuation model which represents the cross section function statistics as the product of a slow and a fast fluctuation. That is,

$$\sigma_o = \bar{\sigma}_o \cdot S \cdot F \qquad (12)$$

The fast fluctuation, F, represents the "instantaneous" Bragg scattering from the capillary waves, while the slow fluctuation, F, represents the variations in the average backscatter strength of the capillary waves due to local surface tilting and wind gusts.

Table IX. Compar'son of the TAGSEA Third Order Model with Sodergren's Model

	TAGSEA	Sodergren
Rapid Fluctuation:		
o Statistics	Slightly Non-Rayleigh	Rayleigh
o Correlation	Independent	Dependent on SS and λ
Slow Fluctuation:		
o Statistics	Normal	Log Uniform or Log Normal
o Correlation		
o Space	Exponential	Constant
o Time	Exponential	Constant

Table IX gives a qualitative comparison between the TAGSEA model and Sodergren's model. As indicated by the table, the details of the two models differ in that the assumed distribution functions and correlation functions are different. However, quantitative comparisons should be made before any conclusions can be drawn.

First consider the slow fluctuation model correlation functions. Neither model is definitive in this respect. Sodergren's model assumes short processing segments and times which are localized in space; thus the long term, large spatial, variations of the fluctuations were not considered. TAGSEA gives a tentative model based on a relatively small amount of supporting data. The model assumes temporal correlation times of 3-10 seconds and spatial correlation distances of 90 to 300 m. High resolution radar sets with resolution cells on the order of 15 to 30 m which perform required CFAR averaging on 10 to 20 cells should not be greatly sensitive to either model. Radar sets which average over larger areas should be evaluated against the TAGSEA model since it provides a more difficult test than the Sodergren model.

Next, consider the statistics of the long term fluctuations. For small variance of the long term fluctuation, the normal, log normal, and log uniform distributions do not differ significantly. Sodergren shows that the relation between the standard deviation of the slow fluctuations, σ_s, and the composite standard-deviation-to-mean ratio, SDMR, is given by

$$\sigma_s = [1/2\ (SDMR^2 - 1)]^{1/2}$$

for a time varying Rayleigh distribution. This result does not depend on the distribution of S. Thus for σ_s = .1 and .2 one gets

SDMR = 1.01 TAGSEA typical
= 1.04 TAGSEA extreme

Sodergren gives SDMR versus grazing angle and sea state. This is given as Figure 3.2-16 and the TAGSEA SDMR as computed above are marked. This figure indicates that the TAGSEA model would produce a low value for the fluctuation statistics. Note, however, such a comparison is not accurate.

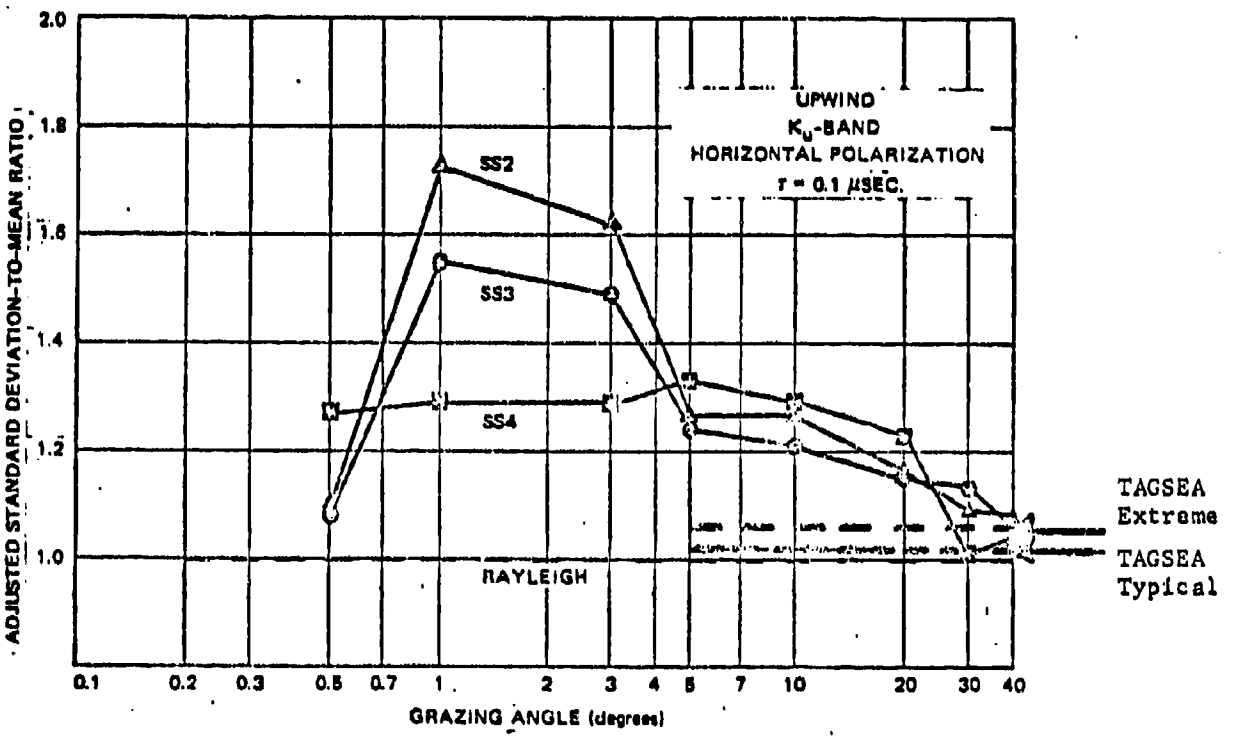

Figure 3.2-16. Adjusted Standard Deviation-to-Mean Ratio.
(From Sodergren [8])

As an example, for run 702, which corresponds to the extreme TAGSEA model for horizontal polarization, the SDMR computed directly from the data is

$$SDMR_{102} = 1.405$$

The apparent contradiction lies in the fact that the TAGSEA model is a time varying non-Rayleigh distribution. Thus the TAGSEA model takes most of the fluctuation out of the slow fluctuation portion and puts it into the rapid fluctuation. As noted earlier in the theoretical discussion, this is primarily a philosophical point. In any practical system, the extreme difficulty of drawing samples from the <u>same</u> resolution cell under <u>identical</u> conditions makes it nearly impossible to physically observe the underlying Rayleigh distribution. Thus correctly using either model should produce equivalent CFAR designs and performance valuations.

Note that the correct application of a time varying Rayleigh model requires sampling from slightly different resolution cells as usually happens in actual data acquisition. This is a subtle point in the application of the time varying Rayleigh distribution which can be overlooked. The TAGSEA model is somewhat preferred since it has already included some of this fluctuation into the rapid fluctuation model.

The rate of rapid fluctuations is different between Sodergren's model and the TAGSEA model. The TAGSEA model assume "white" rapid fluctuations while Sodergren's model assumes the bandwidth of the fluctuations are given by

$$BW = \frac{1.5\ SS}{\lambda}$$

where λ is rf wavelength and SS is hydrographic sea state. At sea state 5, and X band, Sodergren's model gives

$$BW = 250\ Hz$$

At the TAGSEA FFT frame rate ($\approx$ 100 Hz), this corresponds to independent samples frame-to-frame. Thus within the measurement limitations both models agree.

It should be noted that from the theoretical discussion given earlier, for high speed radar platforms, the bandwidth of the fluctuations should be governed by wave motion, the radar resolution cell and the motion of the platform relative to that cell. This is in contradiction to Sodergren's model (which assumes that the bandwidth is governed by sea state) and the TAGSEA model which assumes the rapid fluctuations are white. The latter assumption is safe for low-data-rate systems, but for high-data-rate systems the shape of the fast component, autocorrelation function (or spectrum) may be important. For both situations, the slow component can contribute appreciable to the distribution statistics.

As a final point, it should be noted that the TAGSEA fluctuation model is independent of sea state and grazing angle. This is consistent with the TAGSEA data as illustrated in Table X. There the data sets are grouped such that only sea state varies within a group. Note that generally (except for runs 401 and 403), the effect of sea state and grazing angle is small. Thus the TAGSEA model is consistent relative to its data set. Sodergren shows that the standard-deviation-to-mean ratio varies as a function of grazing angle and sea state (see Fig. 3.2-16). However, for grazing angles above 20°, the effect is not significant. At low grazing angles both Sodergren's data and Bishop's data exhibit fairly strong sea state effects. Thus the TAGSEA model should only be applied at moderate grazing angle and high sea state.

Table X. Effect of Sea State in the TAGSEA Data.

Group	FLT/Run	Parameters	Sea State	10^{-1}	10^{-2}	10^{-3}	10^{-4}	10^{-5}	10^{-6}
I	401	V,1.1,U	3	4.1	7.3	9.3	10.9	12.4	15.0
	1601		4	3.8	7.1	9.1	10.6	11.9	12.9
	Diff.			.3	.2	.2	.3	.5	2.1
II	602	V,1.1,D	5-6	3.9	7.4	9.6	11.3	12.6	13.8
	1602		4	3.8	7.2	9.3	10.9	12.4	13.8
	Diff.			.1	.2	.3	.4	.2	0
III	403	V,1.1,C	3	3.8	7.2	9.5	11.6	13.6	15.4
	603		5-6	3.7	7.1	9.2	10.9	12.3	13.8
	1603		4	3.9	7.1	9.1	10.7	12.0	12.9
	Diff.			.2	.1	.4	.9	1.6	2.5
IV	604	V,2.2,U	5-6	3.8	7.0	9.0	10.5	11.7	12.8
	1604		4	3.9	7.2	9.2	10.8	12.1	13.9
	Diff.			.1	.2	.2	.3	.5	1.1
V	606	V,2.2,C	5-6	3.8	7.2	9.4	11.0	12.4	13.7
	1606		4	3.8	7.2	9.3	11.0	12.3	13.4
	Diff.			0	0	.1	0	.1	.3
VI	1107	V,3.3,U	1	3.8	7.3	9.4	11.0	12.3	13.6
	1607		4	3.7	7.1	9.2	10.8	12.0	13.2
	Diff.			.1	.2	.2	.2	.3	.4
VII	608	V,3.3,D	5-6	3.7	7.1	9.3	10.9	12.2	13.3
	1108		1	3.8	7.3	9.5	11.1	12.6	13.7
	Diff.			.1	.2	.2	.2	.4	.4
VIII	609	V,3.3,C	5-6	3.8	7.2	9.4	11.1	12.4	13.6
	1109		1	3.9	7.4	9.5	11.1	12.3	13.2
	1609		4	3.9	7.4	9.6	11.3	12.7	13.9
	Diff.			.1	.2	.2	.2	.5	.3

1) Table entries are in dB relative to the mean.

4.0 REFERENCES

[1] "TAGSEA Program Final Report: Volume I, Clutter Models", BR-9254-1, Contract N00017-73-C-224, 27 August 1974, Raytheon Company, Missile Systems Division, Bedford, MA.

[2] "TAGSEA Program Final Report: Volume II, Procedures and Output Forms", BR-9254-2, Contract N00017-73-C-224, 27 August 1974, Raytheon Company, Missile Systems Division, Bedford, MA.

[3] "TAGSEA Program Final Report: Volume III, Supportive Analyses and Outputs", BR-9254-3, Contract N00017-73-C-224, 27 August 1974, Raytheon Company, Missile Systems Division, Bedford, MA.

[4] "TAGSEA Program Final Report: Volume IV, Standard Clutter Analysis Outputs", BR-9254-4, Contract N00017-73-C-224, 27 August 1974, Raytheon Company, Missile Systems Division, Bedford, MA.

[5] Pierson, W. J. and R. A. Stacy, "The Elevation, Slope, and Curvature Spectra of a Wind Roughened Sea Surface", NASA Contractor Report, NASA CR-2247, National Aeronautics and Space Administration, Washington, D.C., December 1973.

[6] Trunk, G. V. and S. F. George, "Detection of Targets in Non-Gaussian Sea Clutter", IEEE Trans., Vol. AES-6, No. 5, September 1970, pp. 620-628.

[7] Schmidt, K. R., "Statistical Time-Varying and Distribution Properties of High-Resolution Radar Sea Echo", NRL Report 7150, Naval Research Laboratory, Washington, D. C., 9 November 1970.

[8] Sodergren, P. R., "A Revised K_u-Band Sea Clutter Model", APL Internal Memo, MPD-72U-33, Johns Hopkins Applied Physics Laboratory, Howard County, Maryland, 18 July 1972.

[9] ---, "Presentation on S-Band Sea Clutter Measurements", Private Communication to F. E. Nathanson by Tom Havig, Boeing Co., Seattle, Washington, Summer 1976.

[10] Bishop, G., "Amplitude Distribution Characteristics of X-Band Radar Sea Clutter and Small Surface Targets", RRE Memo No. 2348, Royal Radar Establishment, Great Britain.

[11] Rivers, W., "Low-Angle Radar Sea Return at 3mm Wavelength", Final Technical Report, Project A-1268, Contract N62269-70-C-0489, Georgia Institute of Technology, Engineering Exploration Station, Atlanta, Georgia, 15 November 1970.

[12] Swiff, C. T. and W. L. Jones, "Satellite Radar Scatterometry", IEEE Intercon, 1974.

[13] Peake, W. H. and T. L. Oliver, "The Response of Terrestrial Surfaces at Microwave Frequencies", Technical Report AFAL-TR-70-301, The Ohio State University Electro Science Laboratory, Dept. of Electrical Engineering, Columbus, Ohio 43212, May 1971.

[14] Barrick, D. E., "Radar Clutter in an Air Defense System, Part I: Clutter Physics", Report No. RSIC-798 (AD 834 960L), Contract No. DAAH01-67-C-1921, Battelle Memorial Institute, 505 King Avenue, Columbus, Ohio 43201, January 1968.

[15] Barrick, D. E. and W. H. Peake, "Scattering From Surfaces with Different Roughness Scales: Analysis and Interpretation", Contract No. DA-49-083-OSA-3176, Battelle Memorial Institute, Columbus Laboratories, November 1967.

[16] Horton, C. W. and T. G. Muir, "Theoretical Studies on the Scattering of Acoustic Waves from a Rough Surface", JASA, Vol. 41, No. 3, 1967, pp. 627-634.

[17] Rice, S. O., "Reflection of E. M. Waves by Slightly Rough Surfaces", Theory of Electromagnetic Waves, Interscience 1963.

[18] Ruck, G. T., D. E. Barrick, W. D. Stuart and C. K. Krichbaum, Radar Cross Section Handbook, Plenum Publishers, New York, 1970.

[19] Bradley, G. A., "Remote Sensing of Ocean Waves Using a Radar Scatterometer", Technical Report 177-22, The University of Kansas Center for Research, MSC, NASA Contract NAS-9-10261, 1971.

[20] Guinard, N. W. and J. C. Daley, "An Experimental Study of a Sea Clutter Model", Proc. IEEE, Vol. 58, No. 4., April 1970, pp. 543-550.

[21] Tong, P., "Surveillance Radar Environmental Model", Section 3 of "Electronic Systems Synthesis" given at the Second Annual Conference on Research in System Theory. Sponsored by the Naval Electronic Systems Command, at the Naval Electronic Laboratory Center, San Diego, CA, 22 February 1972.

[22] Trunk, G. V., "Radar Properties of Non-Rayleigh Sea Clutter", IEEE Trans., Vol. AES-8, No. 2, March 1972, pp. 196-204; also, "Modification of 'Radar Properties of Non-Rayleigh Sea Clutter'", IEEE Trans., Vol. AES-9, No. 1, January 1973, p. 110.

[23] Kalbaugh, D. V., "An Engineering Model for Atmospheric Winds", Johns Hopkins Laboratory Internal Memo MPD72U-004, Howard County, MD, 19 January 1972.

[24] Wright, J. W., "A New Model for Sea Clutter", IEEE Trans., Vol AP-16, No. 2, March 1968, pp. 217-223.

[25] Brooks, L. W. and P. R. Brooks, "Further Sea Clutter Data from Previous Tests", Memo No. TSC-W2-68, B50711, Technology Service Corporation, Silver Spring, MD, 21 June 1974.

[26] Daley, J. C., W. T. Davis, and N. R. Mills, "Sea Return Standard", NRL Report 2066, Naval Research Laboratory, Washington, D. C. 21 November 1969.

[27] Daley, J. C., "Radar Backscatter Study at Four Frequencies", NRL Interim Report 5270-20A:JCD:bjg, RO2-37, Naval Research Laboratory, Washington, D. C., 23 August 1966.

[28] Sittrop, Ir. H., "Some Sea-Clutter Measurements, Carried Out from the West-Coast of Norway (Stadt)", Draft Report, Physics Laboratory of the National Defence Research Organization TNO

[29] Nathanson, F. E. and L. W. Brooks, "Quarterly Report on TAGSEA Clutter Test Evaluation", Memo No. TSC-WO-259, Technology Service Corporation, Silver Spring, MD, 20 July 1976.

[30] Brooks, P. R. and L. W. Brooks, "Data Points for K_u-Band Sea Reflectivity", Memo No. TSC-W2-71, Technology Service Corporation, Silver Spring, MD, 19 July 1976.

[31] Brooks, L. W., "Preliminary Comparison of TAGSEA Preliminary Results with Previous Data", Report No. TSC-W2-66, Technology Service Corporation, Silver Spring, MD, 10 May 1976.

[32] Nathanson, F. E. and L. W. Brooks, "Quarterly Report on TAGSEA Clutter Test Evaluation", Memo No. TSC-WO-235, Technology Service Corporation, Silver Spring, MD, 27 April 1976.

[33] Nathanson, F. E. and L. W. Brooks, "Initial Reactions - Raytheon TAGSEA Tests", Memo No. TSC-WO-214, Technology Service Corporation, Silver Spring, MD, 5 March 1976.

[34] Daley, J. C., W. T. Davis and N. R. Mills, "Radar Sea Return in High Sea States", NRL Report 7142, Naval Research Laboratory, Washington, D. C., 25 September 1970.

[35] Brennan, K. M., "Additional K_u-Band and X-Band Sea Clutter Data", Internal Memo MPD72U-034, Johns Hopkins University/Applied Physics Laboratory, Howard County, MD, 19 July 1972.